AD-A136 558 PLASMA MODIFICATION OF GRAPHITE FIBERS AND ITS EFFECT ON COMPOSITE PROPERTIES(U) TUFTS UNIV MEDFORD MASS G DAGLI ET AL AUG 83 AMMRC-TR-83-46 DAAG46-80-C-0057 1/1

UNCLASSIFIED F/G 11/4 NL

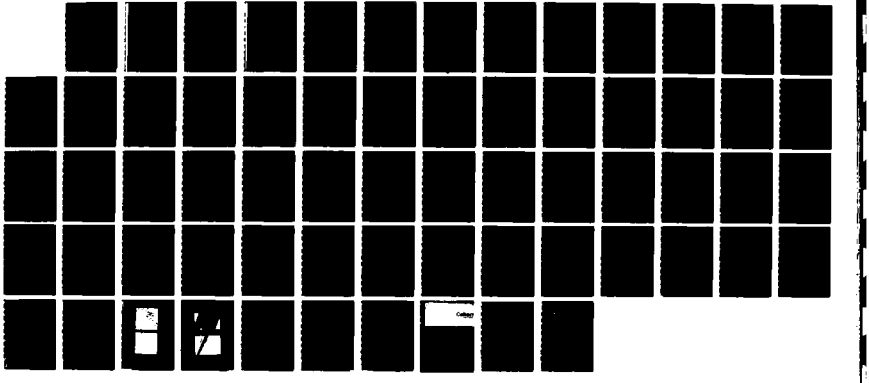

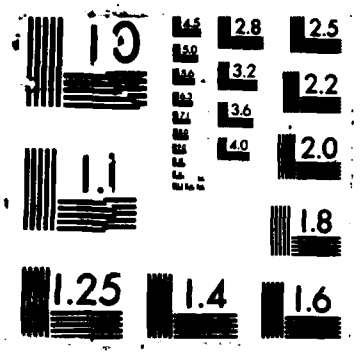
2.8
2.5
3.2
2.2
3.6
2.0
4.0
1.8
1.1
1.25
1.4
1.6

AMMRC TR 83-46

PLASMA MODIFICATION OF GRAPHITE FIBERS AND ITS EFFECT ON COMPOSITE PROPERTIES

August 1983

G. DAGLI and N. H. SUNG
Tufts University
Medford, Massachusetts 02155

FINAL REPORT Contract No. DAAG46-80-C-0057

Prepared for

ARMY MATERIALS AND MECHANICS RESEARCH CENTER
Watertown, Massachusetts 02172

The findings in this report are not to be construed as an official Department of the Army position, unless so designated by other authorized documents.

Mention of any trade names or manufacturers in this report shall not be construed as advertising nor as an official indorsement or approval of such products or companies by the United States Government.

DISPOSITION INSTRUCTIONS

Destroy this report when it is no longer needed.
Do not return it to the originator.

UNCLASSIFIED

SECURITY CLASSIFICATION OF THIS PAGE (When Data Entered)

REPORT DOCUMENTATION PAGE		READ INSTRUCTIONS BEFORE COMPLETING FORM
1. REPORT NUMBER AMMRC TR 83-46	2. GOVT ACCESSION NO.	3. RECIPIENT'S CATALOG NUMBER
4. TITLE (and Subtitle) PLASMA MODIFICATION OF GRAPHITE FIBERS AND ITS EFFECT ON COMPOSITE PROPERTIES		5. TYPE OF REPORT & PERIOD COVERED Final Report - Sept 1980 to June 1982 6. PERFORMING ORG. REPORT NUMBER
7. AUTHOR(s) G. Dagli and N. H. Sung		8. CONTRACT OR GRANT NUMBER(s) DAAG46-80-C-0057
9. PERFORMING ORGANIZATION NAME AND ADDRESS Tufts University Medford, Massachusetts 02155		10. PROGRAM ELEMENT, PROJECT, TASK AREA & WORK UNIT NUMBERS D/A Project: 612105 2571
11. CONTROLLING OFFICE NAME AND ADDRESS Army Materials and Mechanics Research Center ATTN: DRXMR-K Watertown, Massachusetts 02172		12. REPORT DATE August 1983 13. NUMBER OF PAGES 58
14. MONITORING AGENCY NAME & ADDRESS(if different from Controlling Office)		15. SECURITY CLASS. (of this report) Unclassified 15a. DECLASSIFICATION/DOWNGRADING SCHEDULE

16. DISTRIBUTION STATEMENT (of this Report)

Approved for public release; distribution unlimited.

17. DISTRIBUTION STATEMENT (of the abstract entered in Block 20, if different from Report)

18. SUPPLEMENTARY NOTES

19. KEY WORDS (Continue on reverse side if necessary and identify by block number)

Composite materials
Surface chemistry
Mechanical properties
Acrylonitrile polymers
Plasma generators
Carbon fibers

20. ABSTRACT (Continue on reverse side if necessary and identify by block number)

(SEE REVERSE SIDE)

DD FORM 1 JAN 73 1473 EDITION OF 1 NOV 65 IS OBSOLETE

UNCLASSIFIED

SECURITY CLASSIFICATION OF THIS PAGE (When Data Entered)

Block No. 20

ABSTRACT

A new method is explored to improve mechanical properties of carbon/graphite (C/G) fiber reinforced composites through chemical modification of the fiber surface. C/G fiber surface was altered by plasma polymerization of acrylonitrile. Modified surface was characterized with ESCA, FTIR, SEM, and wetting angle measurements, using a pyrolytic graphite block as a model surface to C/G fiber. Acrylonitrile plasma treatment permanently changed the graphite surface to a more polar one with a critical surface energy for wetting, γc, of 54 dynes/cm. Compared to unmodified fibers, plasma treated C/G fiber resulted in substantial improvements in both interlaminar shear and flexural strengths when incorporated uniaxially in epoxy matrices.

FOREWORD

The work described in this technical report was supported by D/A Project number 612105 2571, entitled "Environmental Fatigue Interactions in Fiber Reinforced Composites".
The technical supervisor was Dr. Richard Shuford, Army Materials and Mechanics Research Center, Watertown, Mass. 02172.

TABLE OF CONTENTS

	Page Numbers
Title Page	i
Abstract	ii
Foreword	iii
Table of Contents	iv
List of Tables	v
List of Figures	vi
I. Introduction	1
II. Literature Reviews	3
III. Experimental	9
Materials	9
Plasma Equipment	9
Sample Preparation	10
Surface Characterization	10
Composite Fabrication and Testing	11
IV. Results and Discussion	12
Optimum Conditions for Treatment	12
Post Treatment Condition	13
Surface Characterization of Graphite Block	15
Contact Angle Measurements	15
ESCA	15
SEM	16
IR	16
Mechanical Properties of Composites	17
V. Summary and Conclusions	19
References	21
Appendix	53

LIST OF TABLES

Table 1	Surface Treatment of Graphite Fibers.
Table 2	Flow RAte Effects on Plasma Film Formation.
Table 3	Contact Angle Measurements on Glass Slide.
Table 4	Plasma Treatment Time vs Contact Angles.
Table 5	Elemental Ratios in ESCA Peaks of Graphite Block after various Surface Treatments.
Table 6	Contact Angle Measurements of Untreated and Treated Pyrolytic Graphite.
Table 7	Summary of the ESCA Data on Graphite and PAN.
Table 8	Tentative Assignments of Major IR Bands in Plasma Polymerized Acrylonitrile.
Table 9	Tentative Assignments of Major IR Bands in Poly-acrylonitrile.
Table 10	Mechnical Properties of Fortafil 3/ Epon 828 Composites.
Table 11	Mechanical Properties of Fortafil 3/ Epon 825 Composites.
Table 12	Mechanical Properties of Celion GY-70/ Epon 825 Composites.

LIST OF FIGURES

Figure 1	Surface Energy Relationship at the Liquid-Solid Interface.
Figure 2	The Rate of Plasma Polymerization of Tetrafluoroethylene as a function of Power.
Figure 3	The Rate of Plasma Polymerization of Ethane as a function of Discharge Frequency.
Figure 4	Rates of Plasma Polymerization of Acetylene, Ethylene and Ethane as a function of Monomer Flow Rate.
Figure 5	Rates of Plasma Polymerization of Ethylene, Propylene and Isobutylene as a function of Monomer Flow Rate.
Figure 6	Rates of Plasma Polymerization of Butadiene, Cis-2-Butene and Isobutylene as a function of Monomer Flow Rate.
Figure 7	Characteristic Map for Plasma Polymerization of Ethylene.
Figure 8	Schematic Diagram of the Plasma Treatment Set-Up.
Figure 9	Diagram of the Compression Mold for Fabrication of Composite.
Figure 10	Determination of the Critical Surface Energy for Wetting, $\gamma_{c,}$ of Glass Slide.
Figure 11	Contact Angle Change as a function of Plasma Treatment Time on Glass Slide.
Figure 12	Critical Surface Energy of Untreated (a) and AN Plasma Treated (b) Pyrolytic Graphite.
Figure 13	ESCA Spectra of Untreated (a) and Treated (b) Graphite Blocks and Treated Silicon (c) Surfaces (Treated with Acrylonitrile Plasma)
Figure 14	ESCA Spectra of Polyacrylonitrile.
Figure 15	SEM Micrographs of Pyrolytic Graphite Surfaces, Untreated (a) and treated (b) with AN Plasma (Magnification 1000X).
Figure 16	SEM Micrographs of Fortafil 3 Graphite Fibers, Untreated (a) and Treated (b), with Acrylonitrile Plasma (Magnifications are 8000X and 7000X respectively).
Figure 17	IR Spectra of Plasma Polyacrylonitrile on KBr Substrate (a), (b) is the Expanded Spectra.
Figure 18	IR Spectra of Polyacrylonitrile.

I INTRODUCTION

The use of carbon/graphite fiber reinforced organic matrix composites for lightweight, high strength/stiffness DOD applications has grown substantially in recent years and the trend is projected to continue with even faster rate through 1980's. Such a growth, however, depends on progresses to be made in a number of areas which include lowering the manufacturing cost of fibers, enhancement of quality control through improved processing technology, better fatigue life and long term stability via new design of fiber-resin interface and finally fiber-resin adhesion. Since the main problem encountered in the use of fibers in resin composites is to establish a fiber surface to achieve maximum adhesion between resin and fiber surface, surface and interface aspects of the carbon/graphite fibers and their composites have been extensively investigated (1-4).

A variety of surface coating and modification techniques have been developed (6-11) to improve interfacial bonding as well as to enhance processibility and handling of fibers. An excellent review on the subject has been made available recently by Delmonte (1) and by Drzal (5).

Some of the common treatments (Table 1) include oxidation of fibers with either liquid oxidizing agents (6), such as concentrated nitric acid, potassium permanganate, sodium hypochlorite and hydrochloric acid or with gaseous media (7) such as air, oxygen and ozone. Generally, oxidation etches the fiber surfaces and yield substantial increase in shear strength. However, improved bonding is accompanied by substantial loss in tensile properties especially in the case of gaseous oxidation (8). Another approach has been the application of various polymeric coatings in the order of 1~2% by wt. of fibers such as phenolics, epoxy and organo-silanes and titanates. These resulted in varying degrees of improvement in adhesion but the control of the thickness of coating has been a potential problem. Solutions of reducing agents have been also used such as $FeCl_3$ or ferrocene (4) to improve the interlaminar shear strength. These treatments result in substantial improvement in shear strength, and for the ferrocene, there was no loss in fiber strength. However, the surface contamination of iron compounds on the fiber surface contributes to high temperature instability. Similar adverse effect such as acceleration of the decomposition of carbon fibers at elevated temperature is also reported when fiber is treated with copper acetate solution (9).

Surface modification via vapor phase deposition has been investigated in which carbon/graphite surface was "whiskerized" by growing crystalline fibers, such as silicon carbide, which provides mechanical bonding sites (10).

Recently Subramanian and Jukuboswhi (11) reported a new approach in surface modification through electrochemical polymerization using several vinyl type monomers such as acrylics, styrene and acrylonitrile. There were moderate improvements in the interlaminar shear strength and the impact strength of composites when prepared from the fibers onto which polymers had been grafted through electroplating.

In this study, we have investigated another approach towards modification of carbon/graphite fiber surfaces using a plasma polymerization technique. This method offers certain advantages over the conventional surface treatment in that it provides a means of tailoring the surface systematically for various purposes with relatively simple operations. This work is primarily on the plasma of acrylonitrile and styrene monomers which are applied to various substrates including graphite fibers.

Due to difficulties in handling graphite fibers, other substrates such as pyrolytic graphite block, glass slide, and silicon chip were utilized to characterize the plasma treated surfaces. Electron Spectroscopy for Chemical Analysis (ESCA), Infrared Spectroscopy (IR) and scanning electron microscope (SEM) were used to examine the surfaces of untreated and of plasma treated graphite fibers and pyrolytic graphite blocks.

The mechanical properties of the composites prepared from untreated, plasma treated, and commercially treated graphite fibers were studied.

II LITERATURE REVIEW

FIBER/RESIN INTERFACE

It is generally believed that chemical interaction between the constituents in a multiphase system is not absolutely required to ensure mechanical integrity of the system. The dispersion forces alone exceed the mechanical strength of composites by several orders of magnitude and therefore are not responsible for the premature failure of a reinforced structural material. Instead, the failure is associated with inadequate wetting of the reinforcing constituent by the polymer. Poor wetting minimizes adhesion since the dispersion force field has an extremely limited range. Furthermore, inadequate wetting promotes entrapment of air or vapor at the interface, thereby creating stress concentration spots in a critical area of load transfer.

The requirements for wetting are expressed in terms of energy relationships for the solid and liquid. When wetting occurs spontaneously, the difference between the free energy of the solid at the solid-vapor interface, γ_{SV}, and the combined surface energies at the solid-liquid interface, γ_{SL}, and at the liquid-vapor interface (γ_{LV}) is greater than zero:

$$S = \gamma_{SV} - (\gamma_{SL} + \gamma_{LV}) > 0 \qquad (1)$$

where S is the spreading coefficient (6) and a measure of the work gained in creating a surface element at the liquid-solid boundary. These relationships are shown in Figure 1.

Wetting behavior is also characterized by the contact angle Θ. Under equilibrium conditions, the net free energy at the SL-, SV-, and LV- interfaces, which results from infinitesimal changes in the area at the solid-liquid boundary, is zero. Thus

$$\gamma_{SL}dA + \gamma_{LV}dA\cos\Theta - \gamma_{SV}dA = 0 \qquad (2)$$

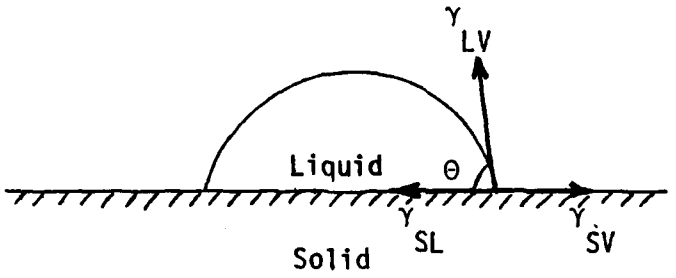

Figure 1 Surface Energy Relationship at the Liquid-Solid Interface

and

$$\cos \Theta = \frac{\gamma_{SV} - \gamma_{SL}}{\gamma_{LV}} \qquad (3)$$

where γ represents the surface energy of the interfaces indicated, and dA the change in surface area. According to equation (3), the wettability increases for those substances for which the equilibrium conditions shift toward larger values of cos Θ . Therefore, the contact angle measurements have generally been used as a means to measure the wettability of the substrate.

Because of the geometry and the very small diameters of graphite fibers, contact angles between fiber and liquids have been difficult to measure with adequate accuracy. As a result, critical surface energy data are not readily available.

A flotation method has been suggested as a means of measuring the critical surface energy of fiber materials [12] . In this procedure the surface tension of the solid is determined by establishing the surface tension of the liquid that just permits the fiber to sink. This is considered to be the critical

surface tension of the fiber surface. However, the fiber density must always exceed the density of the flotation liquid. Although this is a very useful technique, it is inapplicable to graphite fiber due to its irregular surface structure, small filament diameter and small difference in density with flotation liquids.

In view of the difficulties encountered, a different substrate was utilized to study the wetting behavior of the plasma treated surface.

PLASMA AND PLASMA POLYMERIZATION

A plasma is defined as ionized gas consists of atoms, molecules, ions, metastables and excited states of these, and electrons such that the concentration of positively and negatively charged species are roughly the same. The technique of most interest to plasma polymerization is the "cold-plasma" in which free electrons gain energy from an imposed electrical field, and subsequently looses it through collisions with neutral molecules in the gas. The transfer of energy to gas molecules leads to the formation of a host of chemically reactive species, some of which become precursors to the plasma polymerization reaction.

The plasma created by a glow discharge possesses average electron energies in the range of 1 to 10 eV and electron densities of 10^9 - 10^{12} per cubic centimeter [13]. In addition, the electron temperature, T_e of the plasma is not equal to the gas temperature T_g, but has a ratio of 10 to 100. It is therefore possible for plasma polymerization to proceed at near ambient temperature in the presence of electrons to rupture covalent bonds in the gas molecules. Thus, plasma produced by the glow discharge method, called "cold-plasma", is most often used.

The mechanism and kinetics of plasma polymerization have been studied and reported by many (13,14,15,16). One of the common tasks has been to identify the dominant species that control the mechanism of plasma polymerization. Westwood (17) suggested that positive ions from the plasma cause the polymerization reaction to occur. Later, Thompson and Mayham (18,19) supported the cationic mechanism. Recently, Smolinsky and Vasile (20,21) carried out a series of experiments in direct sampling of ionic and neutral species from RF discharges of organic and organometallic vapors, and concluded that highly unsaturated ions play a predominant role.

On the other hand, Denaro et al. (22) favored the free radical mechanism, based on the observation that a significant amount of free radicals are trapped

in the film. The presence of large concentrations of free radicals has also been detected by ESR (electron spinning resonance) technique (23,24,25). Although no experimental data are available for organic plasmas itself, it has been shown that in inorganic systems, free radicals are present to the extent of 10^{-2} to 10^{-1} of the neutral species, whereas ions are present to the extent or 10^{-6} to 10^{-5} of the neutrals (26). This observation is considered reasonable since the energy required to form free radicals (3 - 4 eV) is considerably less than that required to form ions (9 - 13 eV). Therefore, a substantially higher concentration of radicals than ions may be expected. Polymerization is believed to proceed through propagation of radical intermediates and chain growth is terminated by radical recombination (27,28).

Plasma polymerization can be initiated by either pulse or continuous glow discharge. However, the mechanisms of the two methods differ considerably (29). Pulse plasma polymerization is similar to the conventional polymerization process, including the radiation-induced polymerization. During the glow period, initiation process occurs; during the off period, propagation of monomer addition occurs. The end product of the pulsed process is the same as the conventionally polymerized polymer. However, in continuous plasma polymerization, a highly cross-linked polymer is formed which is completely different from the conventionally polymerized polymer. Also, it could be a polymer that has different functional groups than the monomer (30).

For surface modification of graphite fibers, continuous glow discharge mechanism is considered more favorable because it can provide surfaces coated with high cross-linking density polymer. Also, this could enhance a strong cohesive bonding,i.e, grafting between plasma polymer and the substrate, and inhibit intermolecular diffusion of moisture.

The kinetics of plasma polymerization depends on a number of parameters. For a system based on an induction coupled RF electrodeless reactor, some of the key parameters are; power input, substrate location, RF frequency, pressure monomer flow rate, reactor configuration, type of monomer gases, and exposure time.

The rate of plasma polymerization generally increases with increasing power, until at high power densities where the polymerization rate becomes independent of power (31). Figure 2 illustrates the typical power effects on the deposition rate. Although the high power favors the rate of plasma polymerization, it also

accelerated the degradation process at the surface of the substrate. This surface degradation is due to the excess energy carried by the metastables, excess ions, electrons and free radicals, which increases the possibility of knocking off the surface molecules of the substrate. Therefore, for surface modification by plasma polymerization, a moderate power is required to achieve a reasonable deposition rate and minimal degradation. Power also governs the overall area of glow region within the reactor chamber. And it is in the glow region where the maximum rate of polymerization occurs (32).

The kinetics of plasma polymerization is often affected by reactor configuration (33,34,35). Kobayashi (34) showed that under otherwise identical conditions, the polymerization rates of ethylene are not the same for those using tubular type and for bell-jar type reactors. Moreover, electrodeless glow discharge also produces different deposition rates than those with internal electrodes (35).

Plasma polymerization can be carried out in either DC or AC discharge at various frequencies. In DC glow discharge (37), the reproducibility of films deposited is generally poor and also there is often the danger of contamination from sputtering. Therefore, DC discharge is seldom used. In AC glow discharge, the frequency affects the polymerization rate as shown in Figure 3.

Yasuda (38) surveyed 28 different monomers and found that monomers containing aromatic groups, nitrogen (eg. -NH , -NH, -CN), silicon and olefinic double bonds are more readily polymerizable while those containing oxygen (eg. -C=O, -O-, -OH), chlorine, aliphthic hydrocarbon and cyclic hydrocarbons tend to decompose. The latter was confirmed by M.K. Tse (30) who used methylmethacrylate to modify graphite fiber surface. The Fourier Transform Infrared study of the methylmethacrylate plasma modified graphite fibers surface reveals the absence of the carbonyl group. This supports the decomposition tendency of the oxygen containing monomer.

Brown (39) reported in his study of a series of vinyl halides that the dihaloethylenes polymerize more rapidly than the corresponding monohalides, and that chlorides and bromides polymerize more rapidly than the fluorides. Kobayashi (31) found that the additions of certain halogenated compounds to hydrocarbon monomer streams often dramatically increase the polymerization rate. Thus, these halogenated compounds may be considered as gas phase catalysts for the plasma polymerization of hydrocarbons.

Flow rate is one of the key parameters affecting the kinetics of plasma polymerization and the structure of plasma generated films. Generally speaking, at

low flow rates, there is a relative abundance of reactive species so that polymerization rate is limited only by the availability of monomer supply. At high flow rates, however, there is an overabundance of monomer and the polymerization rate then depends on the residence time. At intermediate flow rates, however, the two factors result in a maximum deposition rate. In addition, depending on the reactivity of the monomer itself, different rates were observed (40). Figure 4 through Figure 6 illustrate the above phenomena.

Variations in operating parameters often produce significant differences in the structure and properties of the plasma polymer. For a given monomer in a reactor at a fixed frequency, a "characteristic map" can be constructed (40,41,43) as shown in Figure 7. For ethylene polymerized at a frequency of 13.56 MHz, both powder and film are formed at low pressure and low monomer flow rates (43). At high pressures and high flow rates, an oily product is produced. Only at low pressure and high flow rate can a solid, pinhole-free film be obtained. If the pressure in the reaction is high and the monomer flow rate is low, then the discharge becomes unstable. Furthermore, Figure 7 shows that lower power renders it possible to produce a film at lower flow rates. For conditions near the vicinity of the powder-film border-line, the films are not transparent because of the incorporation of very fine powder particles (44,45). Upon increase of the flow rate, a transparent film can be formed indicating that either powdering product is not formed or powder trapped in the film must be smaller than the wavelength of the visible light. This is the product normally desired for various surface modification.

III EXPERIMENTAL

MATERIALS

A number of substrates were used for plasma modification which include pyrolytic graphite blocks, microscope glass slides, silicon chips and carbon/graphite (C/G) fibers. Pyrolytic graphite blocks were obtained from Pfizer and they were employed as a model substrate for C/G fiber in order to facilitate the use of different surface characterization tools such as contact angle measurements. Surface of the block is parallel to the basal plane of the graphite within several degrees. Graphite blocks were mechanically polished, washed and dried under vacuum at 100°C overnight before they were reacted with plasma. Glass slides and silicon chips were investigated for the purpose of comparison with graphite blocks. Carbon/graphite fibers used were Fortafil-3 supplied by Great Lakes Carbon Corporation and Celion GY-70 fibers from Celanese Plastics Corp. All untreated, unsized and commercially treated grades were used as received except that all the fibers were dehydrated at 110°C, under vacuum overnight before subjected to modification. The technical data sheets on each product are shown in Appendix.

Acrylonitrile monomer used for plasma polymerization was from Eastman Kodak Co. It contained 35 ppm of P-methoxyphenol as an inhibitor. The selection of this monomer is based on the assumption that acrylonitrile will produce a chemically compatible polymer with polyacrylonitrile-based fiber surfaces. Also according to Yasuda (38), plasma polymerized polyacrylonitrile is hydrophilic in nature and this will provide a surface with a high surface energy.

Resin matrix used in the preparation of composites were Epon 825, and metaphenylenediamine (MPDA or CL) as curing agent from Shell Company and E.I. Dupont de Nemours, respectively. Epon 825 is a light colored epichlorohydrin/bisphenol A type liquid epoxy resin. Curing agent, metaphenylenediamine is a solid at room temperature with a physical appearance of light gray to tan flakes. Another resin system, Epon resin 828 and curing agent agent V-40, both from the Shell Oil Company, were used since they were the most commonly used epoxy system in laboratory scale composite fabrication.

PLASMA EQUIPMENT

A plasma treatment set-up consists of a radio frequency power generator (1.5 Kw, 13.56 MHz) from Materials Research Corporation in New York, an impedance matching box by Nye Company in Washington, a tubular reactor made of Pyrex (3 feet long and

4" diameter) coupled with an induction coil outside, a monomer evaporator with flow meters and two vacuum pumps. Over-all layout of the system is shown schematically in Figure 8. Two mechanical vacuum pumps were used to evacuate the system up to about 0.03 $\pm$ 0.02 mm Hg. The pressure was measured by McLeod Gauge. The monomer feed tank was placed into a temperature controlled water bath to maintain a constant vapor pressure of the monomer. The flow rate of monomer vapor was measured by a flow meter.

SAMPLE PREPARATION

The Fortafil 3 and Celion GY-70 graphite fibers were cut into 6-inch tows, and were secured with 1" masking tapes at both ends on a special rack designed to hold the fibers with the maximum amount of fiber surface exposed for plasma treatment. Secured fibers were dehydrated in a vacuum oven at 100°C overnight, then, stored in a vacuum desiccator until the plasma treatment.

Pyrolytic graphite blocks were mechanically polished with #600 silicon carbide sandpaper, then polished with 0.05 μ $A\ell_2O_3$. They were left in acetone for 10 minutes and dried with nitrogen and finally put into vacuum oven at 100°C for overnight drying. Glass slides were washed with soap, rinsed with distilled water then dehydrated at 105°C under vacuum for 10 hours before subjecting to treatment.

Silicon chips were cleaned by immersing in chromic-sulfuric acid solution at 90°C for 10 minutes, etched with HF for 15 seconds then put into HNO_3 solution at 90°C for 10 minutes. Each time they were rinsed with distilled water. They were dried using nitrogen gas and used immediately.

Plasma treatment was conducted typically at a power input of 30∿50 watts under a pressure of 100 ∿ 200 μm Hg with various monomer flow rates and treatment time. The monomer temperature was about 28°C.

SURFACE CHARACTERIZATION

Changes in surface properties of the samples before and after plasma treatment were characterized by wetting angle measurements, electron spectroscopy for chemical analysis (ESCA), and infrared spectroscopy (IR).

Advancing contact angle measurements were made by the sessile-drop method using model A-100 NRL Contact Angle Goniometer manufactured by Rame-Hart Inc. Critical surface energy of wetting, γ_c, of various surfaces was determined according to Zisman's method (46).

ESCA instrument, manufactured by Physical Electronics, was used for elemental

and chemical identification of the surface composition. In ESCA analysis, it is important to determine the relative concentrations of the various constituent atoms. A generalized expression for the determination of the fraction of any constituent atom in a sample, C_x, can be written as:

$$C_x = \frac{n_x}{n_i} = \frac{I_x/S_x}{\Sigma\, I_i/S_i}$$

where n_x is the number of x-atoms, I_i and S_i are respectively the relative peak area in ESCA spectra and atomic sensitivity factor (ASF) of ith element per unit volume.

In IR measurements, both ATR technique and KBr pellet technique were used to obtain the spectra of the treated surface and that of plasma polymer respectively. KBr pellet was about 1 mm in thickness from which the spectra was obtained in transmission mode.

Treated and untreated surfaces of graphite blocks and fibers are examined by a scanning electron microscope (SEM).

COMPOSITE FABRICATION AND TESTING

Unidirectional composites of Celion GY-70 and Fortafil 3 fibers with epon 825 epoxy were fabricated as follows:

First, fibers cut at 6" length were carefully placed onto a bleed cloth (from West Coast Paper Co., Seattle) which is placed on a glass plate. Epon 825 premixed with MPDA at about 60°C was then poured onto the fibers carefully. Another bleed cloth was placed on top of the fiber layout and excess resin was removed by rolling the fibers between the bleed clothes. This was repeated two more times to ensure complete wetting of the fiber. The fibers were then tow by tow aligned into the grooves of the mold which had been sprayed with MS-122 release agent. A diagram of the mold is given in Figure 9. The molding was carried out under a hot press at 85°C for 2 hours followed by 150°C for about 4 hours. The mold was then aircooled, overnight.

Epon 828/V-40 composites were fabricated similarly except that the molding cycle was 60°C for one hour followed by 100°C for 10 hours for post curing.

Composite laminates were then cut to dimensions of 2½" x ½" x ¼" for flexural test and 1½" x ½" x ¼" for interlaminar shear test.

Flexural and interlaminar shear strengths were measured by three-point bending test using an Instron Testing Machine. Span-to-depth ratios were 4 and 16 for interlaminar shear and flexural tests respectively.

IV RESULTS AND DISCUSSION

OPTIMUM CONDITIONS FOR TREATMENT

The nature of coating generated by plasma polymerization is known to be affected by operating parameters such as power input, monomer flow rate, reactor pressure and the location of the substrate with respect to glow region (13). Initial investigation was, therefore, to select an optimum condition which will yield the most desirable coating, namely, a coherent and transparent one. For this purpose, glass slides were used as a substrate. Substrate location was chosen to be inside the glow region where maximum deposition rate was reported by Yasuda (32). Major consideration was to find a condition which will avoid formation of either low molecular weight oily film or powdery coating which normally occurs when gas phase polymerization is favored (13).

One of the variables investigated was flow rate. Using an input power of 50 watts, 10 minutes of exposure time and 60 minutes of post-treatment time, various flow rates were examined with respect to the type of products formed on a glass surface. Table 2 shows the typical results found. The results showed that at low flow rates of up to 8 cm^3/min, brown powders were obtained and wetting test by methanol indicated only the top surface had changed. However, when the top surface was wiped with a cloth, the modified surface disappeared. This suggests that the top surface was not truely modified by plasma polymerization, but rather a layer of plasma polymerized powder was settled from the gas phase onto the surface. On the other hand, at high flow rates of 35 cm^3/min or higher, no visual difference was observed compared to untreated glass slides. Wetting tests, however, showed an uniformily modified surface on both sides of the glass slides and also, the surface remained intact after repeated wiping with a cloth. Therefore, at higher flow rates, a coherent transparent film is obtained which is strongly adhered to the surface. This result is consistent with the general trends observed by other investigators as discussed in literature review section. Based on this result, a 35 cm^3/mm (STP) was selected as a standard flow rate for acrylonitrile monomer.

According to Yasuda (35) the rate of polymerization is independent of discharge power in electrodeless glow discharge. Therefore, the minimum power required to generate flow along the reactor was chosen. For the flow rate of about 35 cm^3/min (or about 120 mm Hg monomer pressure), 30 Watts power was sufficient to generate a

stable glow.

Optimum location of substrates was determined by using a short coil which covered about 4 inches of the reactor. This coil was placed at about 5 inches downstream from the monomer inlet. Glass slides were placed along the full length of the reactor. At an acrylonitrile (AN) flow rate of 35 cc/min with 50 Watts of power, these slides were treated for 1 minute, followed by a post-treatment of 60 minutes in AN monomer vapor. These slides were then subjected to wetting tests, and only the slides placed within the glow region showed an improved wetting behavior. This phenomena was also observed by Yasuda (32), who studied the polymerization rate of tetrafluoroethylene at various position in a similar system. Based on this result, the substrate location was selected to be within the glow region.

The other major parameter was to determine the time of treatment. This was determined by measuring the changes in contact angle of the glass slides as a function of treatment time. To do this, the wetting properties of untreated glass slides were determined first. Table 3 summarizes the measured contact angles on glass slides with different liquids having various surface tension values. Fig. 10 shows the plot of cosine of contact angle against the surface tension. From this plot following Zisman's approach (46), the critical surface energy of the glass slide was found to be about 18 dynes/cm.

Table 4 gives the values of contact angle, found with water and glycerol, on glass slides as a function of exposure times in AN monomer plasma, and Figure 11 shows the plot. Initial contact angle of about 30^{o} for untreated surface was sharply reduced to about 7^{o} in 10 minutes, followed by a gradual reduction to 4^{o} in 25 minutes, and then levelled off. This pattern of initial sharp change followed by much slower change in wetting behavior was reported by others as well (53,54). Levelling of the contact angle is assumed to be the on set of the complete coverage of the surface by plasma polymer, which occurs at around 20 minutes of treatment. Based on this data, the plasma treatments were all carried out for 30 minutes.

POST TREATMENT CONDITION

It has been observed that free radicals remain on the substrate surface after the plasma treatment (42,55,25). These active sites are probably formed both through incorporation of free radicals from the gas phase, and by the impingement of active plasma species and radiation onto the deposited film. Due to the highly crosslinked structure, trapped radicals have low mobility and do not recombine

rapidly. Upon exposure to the atmosphere, these radicals react with oxygen and form carbonyl and hydroxyl groups. These radicals were found to posses a long half life (47,48) and have been known to be responsible for polymerization to continue after the plasma has been turned off. Reaction of these trapped free radicals with the surrounding atmosphere can alter the final structure of the surface. Various post treatment conditions were therefore applied to the graphite surfaces immediately after the plasma treatment and their effects on the structure were examined by using ESCA. Post treatment conditions include;

1. 10 hrs. in vacuum
2. 1½ hrs. in monomer gas
3. 4 hrs. in monomer gas
4. 10 hrs. in monomer gas
5. no post treatment (exposed to air immediately)

ESCA data on each surface are summarized in Table 5 where the ratio of major peaks C_{1s}, O_{1s}, and N_{1s} are compared.

Between the samples with no post treatment (i.e., exposed to air immediately after the plasma treatment) and 10 hours in vacuum, both the O/C and the N/C ratios were significantly higher in the former compared to the latter. It appears that the post treatment in vacuum for 10 hours substantially reduces the free radical concentrations and thereby reduces the extent of reaction with oxygen and nitrogen in air. Within the series post treated with acrylonitrile monomer, there were systematic changes in the elemental ratios such that the ratio of O/C decreased with increasing post treatment time while the ratio of N/O showed gradual increase. In other words, relative amount of oxygen with respect to carbon and nitrogen becomes lower with increasing amount of post treatment. This result is consistent with the speculation that during the post treatment, further polymerization of acrylonitrile monomer would proceed by the initiation of the residual free radicals (described as plasma induced polymerization (13)) and this will produce poly-acrylonitrile similar to conventionally produced PAN. As a consequence, the amount of free radicals would be reduced substantially resulting in less amount of oxygen to be incorporated upon subsequent exposure to air. Post treatment with monomer, therefore, seems to produce the surface which will resemble the structure of conventional PAN, at least on the very top layer. When the post treatment of 10 hours vacuum is compared to 10 hours in monomer, the relative amount of oxygen is significantly higher in the former suggesting that during the vacuum treatment, free radicals are noteasily annihilated as when they are exposed to monomer and therefore, subsequent exposure to air results in higher concentrations of oxygen.

Based on the results on the effects of operating variables and post treatment conditions, a standard condition for the AN plasma treatment was established as follows:

Power: 30 Watt
Pressure: 120 mm Hg
Monomer flow rate: 35 cm^3/min
Exposure time: 30 min
Post treatment time: 1.5 hours

SURFACE CHARACTERIZATION OF GRAPHITE BLOCKS

CONTACT ANGLE MEASUREMENTS: Wetting angle of the treated graphite surface was measured with water at 25°C and the value of 5° was obtained which is close to that observed in treated glass surface. This was a drastic change from the untreated surface which was non-wetting with the angle of 82° (Table 6). This indicates that graphite surface becomes much more polar after treated with AN plasma. Another important fact is that this surface is not easily changed by mechanical or by solvent removals, indicating that the surface change is permanent.

Further characterization was made to determine the critical surface energy of wetting, γ_c, of both untreated and treated surfaces by measuring contact angles with a series of test liquids (Table 6) and by Zisman's plot (Figure 12). From Figure 12, the values of γ_c for graphite blocks were found to be $\sim$ 32 dynes/cm for untreated and $\sim$ 54 dynes/cm for treated surface. 32 dynes/cm for untreated pyrolytic graphite surface is close to a reported value of 28 dynes/cm for Pfizer graphite ribbon by Dynes and Kaelble (52).

Increase in γ_c value in AN plasma treated surface make it easy to be wetted by liquids. Improved wetting is also observed with Epon 828 resin as shown in Table 6.

ESCA ANALYSIS: The treated and untreated graphite surfaces were examined with ESCA. Figure 13 shows the ESCA spectra for untreated (a) and treated (b) graphite. Also shown in Figure 13-c is the spectra of the silicon treated under the same condition as graphite for comparison. Table 7 summarized the ESCA peak ratios and elemental ratios of carbon, nitrogen and oxygen atoms. In untreated graphite (13-a), C_{1s} peak was observed at 284.3 eV which corresponds to graphite carbon. Also substantial amount of O_{1s} peak was seen at 530.0 eV, which may arise from surface carbonyl and carboxylic groups. The ratio of C/O was 3.57.

In treated graphite surface (13-b), in addition to C_{1s} and O_{1s} peaks, a strong N_{1s} was present. At high resolution, most peaks appear as multiple peaks: C_{1s} (284.7 - 288.6 eV), O_{1s} (531.9 - 532.5 eV) and N_{1s} (400.4 eV), suggesting that the structure of plasma polymerized acrylonitrile (PPAN) may be quite complicated. The ratio of C/O in treated sample is 1.54 which is much lower than 3.57 of untreated sample and the ratio of N/C is 0.34. In treated silicon (figure 13-c), ESCA peaks are similar to those from treated graphite, showing only C_{1s}, N_{1s} and O_{1s} peaks and no Si peak was detected. This indicates that the silicon surface was completely covered with PPAN at least to a depth of 50 $\sim$ 100 Å.

ESCA of a clean polyacrylonitrile surface is shown in Figure 14 for comparison and the elemental ratios and concentrations in PPAN and PAN are summarized in Table 7. ESCA results clearly show that PPAN contains substantially higher concentrations of both N and O atoms when compared to conventionally produced PAN.

SCANNING ELECTRON MICROGRAPHS: Figure 15 shows the SEM micrographs of the pyrolytic graphite blocks which were polished, untreated (15-a) and treated (15-b) with acrylonitrile plasma. No major difference was detected between the two, suggesting that plasma does not etch the surface. Since the PPAN deposited is not expected to be greater than 1000 Å in thickness, it is unlikely that the surface texture would be altered by such a thin coating. Figure 16 shows the SEM micrographs of both untreated (16-a) and treated (16-b) Fortafil-3 graphite fibers. This fiber is PAN based and the surface is relatively smooth. Again no major differences in surface textures were detected. Plasma treatment appears, therefore, neither to develop any surface etching nor to increase roughness to a significant level.

INFRARED SPECTRA OF PPAN: IR spectra of the plasma polyacrylonitrile were obtained using KBr pellet technique. The KBr powder was treated with AN plasma and the spectra was obtained through transmission mode. The result is shown in Figure 17. Various attempts to obtain spectra directly from AN plasma treated graphite by the ATR technique were not successful due to the insufficient peak intensity to overcome noise problem. The IR spectra of conventional polyacrylonitrile is given in Figure 18. The major IR bands for PPAN and PAN are summarized in Tables 8 and 9 respectively. Band assignments are tentative and based on the published data in the literature (56).

In general, the spectra of PPAN is substantially different from that of PAN. Some major differences are a broad and strong peak at around 3400 cm^{-1}, peaks at 2166 cm^{-1}, 1560 cm^{-1}, 1121 cm^{-1} and 805 cm^{-1} which are present only in PPAN. A broad

peak at 3400 cm^{-1} is probably due to NH peaks as well as OH peaks from moisture, which may be present in KBr Amide II band at 1560 cm^{-1} is clearly seen in PPAN but not present in PAN. Also, relatively strong band at 1120 cm^{-1} indicates the possible presence of high concentrations of OH groups in PPAN. Although further studies are needed to better assign these peaks, it appears that PPAN contains high concentrations of C = O groups and OH groups. This is consistent with the highly polar nature of PPAN surface as determined by wetting angle measurements.

MECHANICAL PROPERTIES OF COMPOSITES

Effect of plasma treatment of fibers on the fiber-resin interaction was investigated by making composites and measuring flexural and interlaminar shear strengths (ILSS). Uniaxial composites of Fortafil-3 graphite fiber/Epon 828 and Epon 825 epoxy resins, containing fibers of ca. 60% by volume, were fabricated and tested. Also uniaxial composites of Celion GY-70 graphite fibers/Epon 825 epoxy were studied. In all composite systems, AN plasma treated fibers are compared with both untreated control and commercially treated grades. Tables 10, 11 and 12 summarize the strength data.

In Fortafil 3 /Epon 828 composites, composites with untreated fibers exhibited the highest flexural strength (148 ksi) and the lowest ILSS (7100 psi). Compared to this both commercially treated and sized (by Great Lakes Carbon Corp.) fibers yielded slightly higher ILSS (7400 $\sim$ 8000 psi), but at a substantial loss of flexural properties (111 $\sim$ 127 ksi). This is typical of many commercially treated fibers where treatment may involve oxidation or surface etching. AN plasma treated fibers, on the other hand, showed a substantial improvement of ILSS (8200 psi) over the control, highest among the four, and this was achieved without any loss of strength.

Table 11 shows the data from Fortafil 3/Epon 825 Composites containing ca. 60% fibers. Again, AN plasma treatment resulted in improved ILSS (7900 psi) over the control (7200 psi) and, more interestingly, a substantial increase in flexural strengths (199 ksi vs 170 ksi). Commercially sized and/or treated fibers showed mixed results, sized fibers being the poorest of all.

In Celion GY-70/ Epon 825 Composites, the highest flexural strength was obtained with AN plasma treated fibers (138 ksi), which is considerably higher than both untreated (112 ksi) and commercially treated grade (123 ksi). Plasma treatment resulted in a 65% increase in ILSS compared to untreated fibers. However, this was not as high as the ILSS values obtained with commercially treated GY-70 fibers.

The overall effect of the AN plasma modification of graphite fibers is that it improves substantially the ILSS and at the same time, improves or maintains the original strength of the untreated fibers. Increase in ILSS of epoxy matrix composites appears to depend on the type of fibers. Improved flexural properties of the AN plasma treated fiber composites may be due to either improved wetting of the treated fibers, as evidenced by wetting experiment, or improved tensile strength of the fiber itself, or both. Preliminary tests indicates that AN plasma treatments enhance the tensile strength of some graphite fibers. It is plausible that plasma polymerization may effectively heal the smaller size surface cracks thereby increasing the strength. (This aspect of the research clearly needs further investigation.) Improvements of of ILSS in Celion GY-70 fibers by plasma were relatively small compared to commercial treatment. This may be due to limited exposure of individual fibers to plasma gas during the treatment because of considerable difficulties in opening the fibers from its bundle of particular tape construction. In other words, only part of the fiber surfaces might have been modified.

V SUMMARY AND CONCLUSIONS

1. Surface modifications of C/G fibers and pyrolytic graphite blocks with acrylonitrile (AN) plasma was carried out in a tubular plasma reactor coupled with a RF indication coil. Optimum operating parameters were determined by monitoring the changes in surface properties with wetting angle measurements. Typical treatment conditions employed are:

   Power input = 30 ∿ 50 watt
   Monomer flow rate = 35 cc/min (STP)
   Treatment time = 10 ∿ 30 minutes
   Monomer Temperature = $28^{o}C$

2. Pyrolytic graphite blocks were used as a model surface to C/G fibers. This allows the use of contact angle measurements as a means of monitoring the surface changes during the plasma treatment and also to obtain the critical surface energy for wetting, γ_c, of the treated and untreated surfaces.

3. AN plasma treated graphite surface is much more polar and thus, more readily wettable (see Table 6). γ_c of untreated graphite surface is 28 ∿ 32 dynes/cm which was increased to about 54 dynes/cm (see Figure 12) and thus wetting by polymeric fluid, such as Epon 828, is greatly enhanced (Table 6)

4. Exposure of treated surfaces to various environments immediately after the AN plasma treatment was investigated. ESCA analyses of the post-treated surfaces suggest that maintaining the treated surface in AN monomer vapor promotes the plasma-induced polymerization of acrylonitrile on the surface, whereas direct exposure to air results in higher concentrations of oxygen and nitrogen atoms in relative to carbon (Table 5).

5. ESCA analyses of treated surfaces reveal that the AN plasma treated surfaces are identical and independent of the type of substrates among graphite, glass and silicon. Also the surface is completely covered by PPAN (Figure 3). Preliminary data of IR spectra suggests

that PPAN contains a number of peaks which are absent in PAN spectra, suggesting that the structure of PPAN is much more complicated. Among the peaks, amide II, carbonyl and OH appears to be abundant in PPAN.

6. SEM micrographs of the treated and untreated surfaces are identical (Figures 15 and 16) in both fiber and block specimens, suggesting that AN plasma has no etching effect under these conditions.

7. AN plasma treated fibers are compared with untreated or commercially treated fibers by making unaxial composites with epoxy matrix and testing interlaminarshear and flexural strengths. With both Fortafil 3 fibers (by Great Lakes Carbon) and Celion GY-70 fibers (by Celanese Plastics Co.), AN plasma treated fibers provided consistently the highest flexural properties among the three types of fibers except for Fortafil 3/828 and also substantially higher interlaminarshear strength compared to untreated fibers. Higher flexural strength appears to be due to improved wetting of the fibers by epoxy matrix and also in part, by enhanced fiber strength by AN plasma.

REFERENCES

1. J. Delmonte, "Technology of Carbon and Graphite Fiber Composites", Chapter 6, Van Nostrand Reinhold Company, (1980).

2. D.A. Scola, in "Composite Materials", Vol. 6, Ed. E.P. Plueddemann, Chapter 7, Academic Press, (1974).

3. D.A. Scola, C.S. Brooks, Journal of Adhesion, 2, p.p. 213-237 (1970).

4. J.V. Larsen, "Surface Treatments and their Effects on Carbon Fibers", Paper and Bibliography, U.S. N.O.L., Silver Springs, Maryland, (1971).

5. L. T. Drzal, Carbon, Vol. 15, p.p. 129-138, (1977).

6. J.C. Goan, "Graphite Fiber Oxidation", Naval Ordinance Laboratory, TR-153. November (1969).

7. H. Nyo, D.L. Heckler and P.L. Hoernschemeyer, SAMPE 24th National Symposium, Vol. 24, p. 51, (1979).

8. R.J. Dauksysis, "Coupling of Epoxy Polymers to Graphite Fibers", AFML 72-23, May, (1972).

9. Chemical Abstract-76-86634P, (1972).

10. J.V. Milewski and J.V. Anderle, GTC Technical Report 127.7-1.

11. R.V. Subramanian and J.J. Jukubowski, Polym. Eng. Sci. 18, 590 (1978).

12. J.P. Mutchler, J. Menkart, and A.M. Schwartz, (1967) National Meeting, Amer. Chem. Soc., Miami, Florida, Div. Colloid Surface Chem., 153rd Abstract 59A.

13. M. Shen and A.T. Bell, "Plasma Polymerization" Ed. M. Shen and A.T. Bell, Ch.1, A.C.S., Washington D.C., 1979.

14. D.T. Clark, A. Dilks and D. Shuttleworth, "Polymer Surfaces" Ed. D.T. Clark, W.J. Feast, Ch.9, Wiley, NY, 1978.

15. A.T. Bell, "Plasma Chemistry of Polymers" Ed. Mitchel Shen, Ch.1, Dekker, NY, 1976.

16. H. Yasuda, "Plasma Chemistry of Polymers" Ed. Mitchel Shen, Ch.2, Dekker, NY, 1976.

17. A.R. Westwood, Europ. Polymer J., 1971, 7, 363.

18. L. F. Thompson, K.G. Mayhan, Appl. Polymer Sci, 16, 2291, 1972

19. L.F. Thompson, K.G. Mayhan, J. Appl. Polymer Sci, 16, 2317, 1972.

20. M.J. Vasile, G. Smolinoky, J. Electrochem. Soc., 119, 451, 1972.

21. G. Smolinsky, M.J.Vasile, J. Macromol. Sci. - Chem., 10, 473, 1976.

22. A.R. Denaro, P.A. Owens, A. Crawshaw, Europ. Polymer J., 4, 93, 1968.

23. H. Kobayashi, M. Shen, A.T. Bell, J. Macromol. Sci. - Chem., 8, 373, 1974.

24. S. Morita, T. Mitzutani, M. Ieda, Jap. J. Appl. Phys. 10, 1275, 1971.

25. N. Morosoff, N. Crist, B.Bumgarner, M., Hus, T., Yasuda, H.J. Macromol Sci. - Chem., 10, 451, 1976.

26. S.W. Benson, H.E. O'Neal, "Kinetic Data on Gas Phase Unimolecular Reactions", NSRDS-NBS21, U.S, Department of Commerce, Washington D.C., 1970.

27. M. Shen and A.T. Bell, Organic Coatings and Plastic Chemistry, Vol. 38, 550, 1978.

28. M. Shen and A.T. Bell, Polymer Reprints, Vol. 19, No.2, 429 - 543,1978.

29. H. Yasuda and T. Hsu, J. of Polym. Sci. - Chem., 15, 81, 1977

30. M.K. Tse, "Plasma Treatments of Graphite Fibers as a measure to improve the interlaminar shear strength of graphite fiber reinforced composites." M.S. Thesis, MIT, Department of Nat'l Sci., 1978.

31. H. Kobayashi, M. Shen, A.T. Bell, J. Macromol. Sci.-Chem., 8,1345,1974.

32. H. Yasuda, N. Morosoff, J. Appl. POlym. Sci., 24, 1033, 1979.

33. M. Millard, "Techniques and Applications of Plasma Chemistry" Ed. J.R. Hollahan and A.T. Bell, Ch.5, Wiley, NY, 1974.

34. H. Kobayashi, A.T. Bell, M. Shen, J. Macromol. Sci.-Chem., 10,491, 1976.

35. H. Yasuda, C.E. Lamaze, J. Appl. Polymer Sci., 15, 2277, 1971.

36. K. Cutfreund, "Modern Composite Materials" Ed. L.J. Brountman, R.H. Krock, Ch.6, Addison-Werley Publishing Co., 1967.

37. A.M. Mearns, Thin Solid Films, 3, 201, 1969.

38. J. Yasuda, C.E. Lamaze, J. Appl. Polym. Sci., 17, 1533, 1973.

39. K.C.Brown, Europ. Polym. J., 8, 117, 1972.

40. H. Kobayashi, A.T. Bell, M. Shen, Macromol., 7, 277, 1974.

41. H. Kobayashi, M. Shen, A.T. Bell, J. Macromol. Sci.-Chem., 8,373, 1974.

42. A.R. Denaro, P.A. Owens, A. Crawshw, Europ. POlymer J., 4, 93, 1968

43. H. Kobayashi, M. Shen, A.T. Bell, J. Appl. Polym. Sci., 18, 885, 1973.

44. L.F. Thompson, G. Smolinsky, J. Appl. Polym. Sci., 16, 1179, 1972.

45. M. Niimomi, H. Kobayashi, A.T. Bell, M. Sehn, J. Appl. Phys., 44, 4317, 1973.

46. W.A. Zisman, "Contact Angle, Wettability and Adhesion", Advances in Chemistry Series 43, Chapter 1, American Chemical Society, Washington (1964).

47. A.K. Sharma, F. Millich and E.W. Hellmuth, "Organic Coatings and Plastics Chemistry", ACS, Vol. 38, March, (1978).

48. M.S. Grenda, M. Venugopalan, Journal of Polymer Science, Polymer Chemistry, Edition 18, p. 1611 (1980).

49. Handbook of X-Ray Photoelectron Spectroscopy, Physical Electronics.

50. Standard Method of Test for apparent horizontal shear strength of reinforced plastics by short-beam method.

51. ASTM Designation: D790-70
Standard Methods of Test for Flexural properties of plastics.

52. P.J. Dynes, D.H. Kaelble, Journal of Adhesion, 6, 195 (1974).

53. C.I. Hammermesh, P.J. Dynes, Polymer Science, Polymer letters, Ed., 13, p. 663 (1975).

54. N.K. Eib, K.L. Mittal, A. Friedrichs, Journal of Polymer Science, 25, p. 2455 (1980).

55. H. Kobayashi, M. Shen, A.T. Bell, Journal of Appl. Polymer Science, 18, 885 (1973).

56. C.Y. Liang and S. Krimm, Journal of Polymer Science, 31, p. 513 (1958).

Table 1 Surface Treatments of Graphite Fibers (5)

Methods	Effects on Mechanical Properties
Oxidation (Wet)	
HNO_3	20-200% increase in ILSS; decrease in tensile strength; effect varies with degree of graphitization and precursor
$KMNO_4$ H_2SO_4	100-200% increase in ILSS; slight decrease in tensile strength and flexural strength
Sodium hypochlorite	30-100% increase in ILSS
Chromic acid	Decrease in tensile strength; excess degradation of fiber
Electrolytic NaOH	70-120% increase in ILSS; slight decrease in tensile strength
Oxidative (Dry)	
Vacuum desorption	20% increase in ILSS
Air	10-200% increase in ILSS; difficult to control
Oxygen or Ozone	20-40% increase in ILSS; difficult to control
Catalytic oxidation	50-100% increase in ILSS
Coatings	
HNO_3 + polymer coating	Slight increase in ILSS (over HNO_3)
Air + alternating & block copolymers	50-100% increase in ILSS
Vapor Phase Deposition	
Pyrolytic C	25-60% increase in ILSS; varies with fiber type
Silica/silicon	Slight increase in ILSS; increase in oxidative resistance
Metals	Increase in oxidative resistance
Whiskerization	
SiC	200-400% increase in ILSS; depends on fiber type

Table 2 Flow Rate Effects on Plasma Film Formation

Pressure = 80 - 150 μm
Power = 50 Watt
Monomer = acrylonitrile
Exposure Time = 10 min.
Post-Treatment Time = 60 min.

Flow rate (cm^3/min)	Type of Product	Surface changes by Wetting tests
1.2	Brown Powder	One Side Only (Top)
5.0	Brown Powder	One Side Only (Top)
8.0	Brown Dust	One Side Only (Top)
20.0	Yellow Brown Dust	Two Sides (bottom side showed only a small change in wetting behavior)
26.0	White Dust	Two Sides
35.0	Transparent	Two Sides (wetting behavior exactly the same on both sides)
45.0	Transparent	Two Sides

Table 3 Contact Angle Measurements on Glass Slide

Test Liquids	γ_{LV}*	Contact Angles (in degrees) θ	Cos θ
Water	72.8	33	0.84
Glycerol	64	30	0.87
Formamide	58.3	27	0.89
Ethylene Glycol	48.3	25	0.91

*Surface tension of test liquid, dynes/cm

Table 4 Plasma Treatment Time Versus Contact Angles on Glass

Monomer = Acrylonitrile

Power = 30 Watts

Post Treatment = 90 Minutes

Monomer Flow Rate = 35 cm^3/min

Treatment Time* (min)	Contact Angles (in degrees) Water	Glycerol	Formamide
1	25-27	17-24	5-7
6	13	11	6
8	6-10	5-6.5	2.5
10	6	6-7	3
20	5-6	4-5	2-3
25	4.5-5	3.5-5	--
30	5	3-5	2-3
50	4.5-5	3-4	wets
75	4	3-4	wets

Table 5 Elemental Ratios in ESCA Peaks of Graphite Block after Various Surface Treatments

Post Treatment*	$\frac{O}{C}$	$\frac{N}{C}$	$\frac{N}{O}$
untreated graphite	0.23	0.00	0.00
no post treatment	0.81	0.91	1.13
1½ hr. w/monomer	0.65	0.34	0.33
4 hr. w/monomer	0.45	0.49	1.10
10 hr. w/monomer	0.38	0.46	1.21
10 hr. vacuum	0.70	0.69	0.98

*Post treatment after treatment with acrylonitrile plasma for 30 minutes with power = 40∿50 watts, monomer flow rate ≈ 35 cc/min, and pressure = 160∿180 μm Hg.

Table 6 Contact Angle Measurements of Untreated and Treated Pyrolytic Graphite

Test Liquids	γ_{LV}*	Contact Angles (In Degrees)	
		Pyrolytic Graphite	Treated Graphite Block
Water	72.8	82	5.5
Glycerol	64	71.5	4.5 ∿ 5
Formamide	58.3	55	3
Ethylene Glycol	48.3	45	-
Polyglycol** P15-200	36.6	21.5	-
Polyglycol** P1200	31.3	12	-
Epon 828***	-	26 ∿ 28	8 ∿ 9

*surface tension of test liquid, dynes/cm

**supplied by Dow Chemical

***testing temperature was 38°C

Table 7 Summary of the ESCA Data on Graphite and PAN

	ESCA Peak Ratio		Estimated Elemental Concentrations (%)		
	$\frac{O}{C}$	$\frac{N}{C}$	C	N	O
Untreated graphite	0.28	0	91	0	9
Treated graphite	0.65	0.34	66	19	15
PAN	0.25	0.17	85	8	7

*Treated with AN Plasma for 30 minutes followed by post treatment with AN monomer for 90 minutes.

Table 8 Tentative Assignments of Major IR Bands in Plasma Polymerized Acrylonitrile (PPAN)

Wave Number (cm^{-1})	Intensity	Possible Source
3430	S	-NH, $-NH_2$ -OH
2960	S	CH stretching (CH_3)
2930	S	CH stretching (CH_2)
2855	W	CH_2
2165	S	CH stretching
1663	S	-C=C-(non conjugated), -C=N (open chain)
1560	W	amide II
1460	W	CH deformation (CH_2,CH_3) branching & x-linking
1380	S	CH_3(branching)
1260	S	(primary alcohol) OH, C=O stretching
1120	S	(primary alcohol) OH, C=O stretching
1030	S	CN stretching (ring system), -C=CN
870	W	aromatic CH, CH deformation
805	S	CH out of plane, C=C

Table 9 Tentative Assignments of
Major IR Bands in Polyacylonitrile (PAN)

Frequency (cm^{-1})	Intensity	Possible Source
2940	strong	$-CH_2$ stretching
2875	medium	$-CH_2$ stretching
2240	strong	C≡N stretching
1670	strong	-C=C, -C=O stretching - NH deformation -C=N stretching
1455	strong	-CH deformation, C=C Skeletal R-N=O, N-N=O
1390	medium	CH deformation
1362	medium	$-CH_2$ wagging
1320	weak	CH bending
1255	medium	-OH deformation, CO stretching
1225	weak	$-CH_2$ twisting
1095	medium	-CO stretching, C-N vibrations CH deformation
1070	medium	C-N vibrations CH deformation C-O vibrations
1040	weak	OH deformation, CO stretching
865	weak	CH out of plane deformation
780	weak	$-CH_2$ rocking
660	medium	≡CH deformation
		CH out of plane deformation

Table 10 Mechanical Properties of Fortafil 3/Epon 828

Composites ($V_f \cong 60\%$)

Fiber treatment	Flexural Strength (ksi)	Interlaminar Shear Strength (ksi)
None*	148 ± 10	7.1 ± 0.5
Commercial treatment**	111 ± 18	7.4 ± 0.5
Commercial Size**	127 ± 15	8.0 ± 0.3
AN plasma (5 min)	145 ± 5	8.2 ± 0.1

* Unsized, untreated

** Treated by Great Lakes Carbon Corp.

+ Span-to-depth ratio 4

Table 11 Mechanical Properties of Fortafil 3/Epon 825 Composites ($V_f \cong 60\%$)

Fiber Treatment	Flexural* Strength (ksi)	Interlaminar Shear Strength (ksi)
None**	170 ± 12	7.2 ± 0.8
Commercial Treatment***	198 ± 10	10.3 ± 0.8
Commercial Sized***	140 ± 13	6.9 ± 0.3
AN Plasma	199 ± 29	7.9 ± 0.3

* Span to depth ratio is 16 to 1.

** Unsized, untreated

*** Treated by Great Lakes Carbon Corp.

Table 12 Mechanical Properties of Celion GY-70/ Epon 825 Composite (V_f= 60)

Fiber Treatment	Flexural* Strength (ksi)	Interlaminar Shear Strength (ksi)
None	112.3 ± 5.4	3.3 ± 0.2
Commercial Treatment**	122.8 ± 5.3	8.1 ± 0.3
ANPlasma	138.0 ± 4.0	5.4 ± 0.3

* Span-to-depth ratio is 32 : 1

** By Celanese Plastics Co.

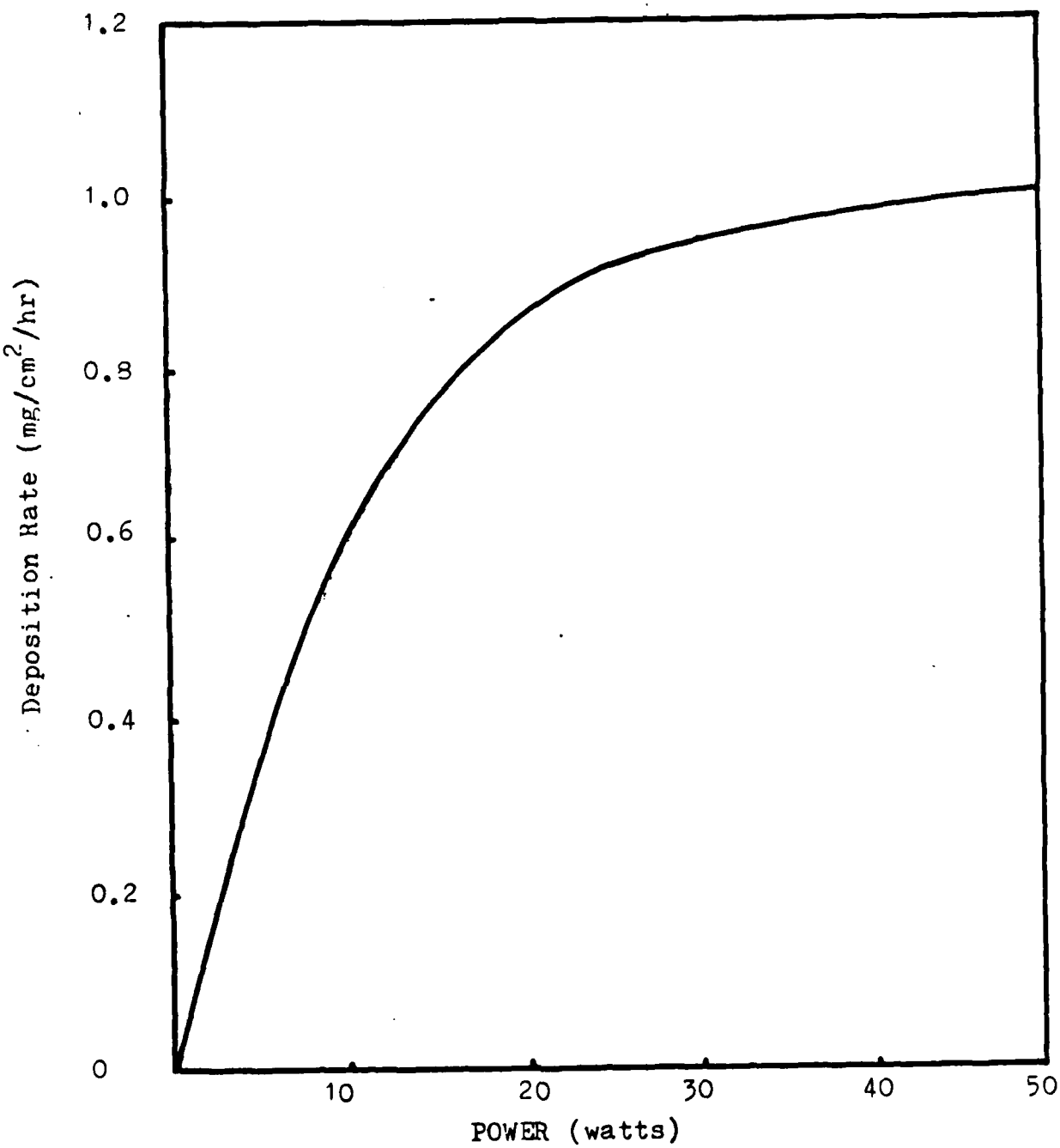

Figure 2: The Rate of Plasma Polymerization of Tetrafluoroethylene as a function of Power (40).

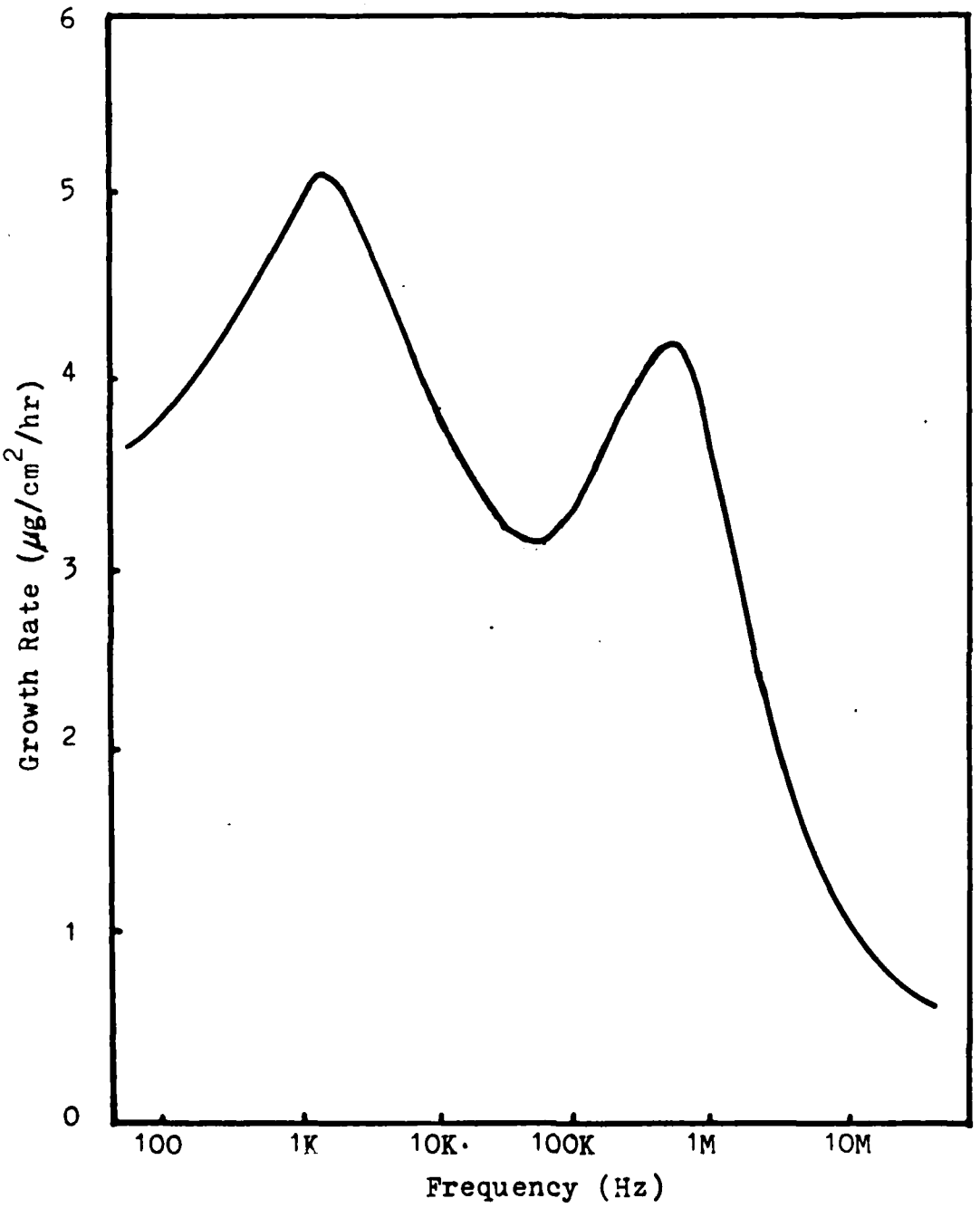

Figure 3: The Rate of Plasma Polymerization of Ethane as a function of Discharge Frequency.(40).

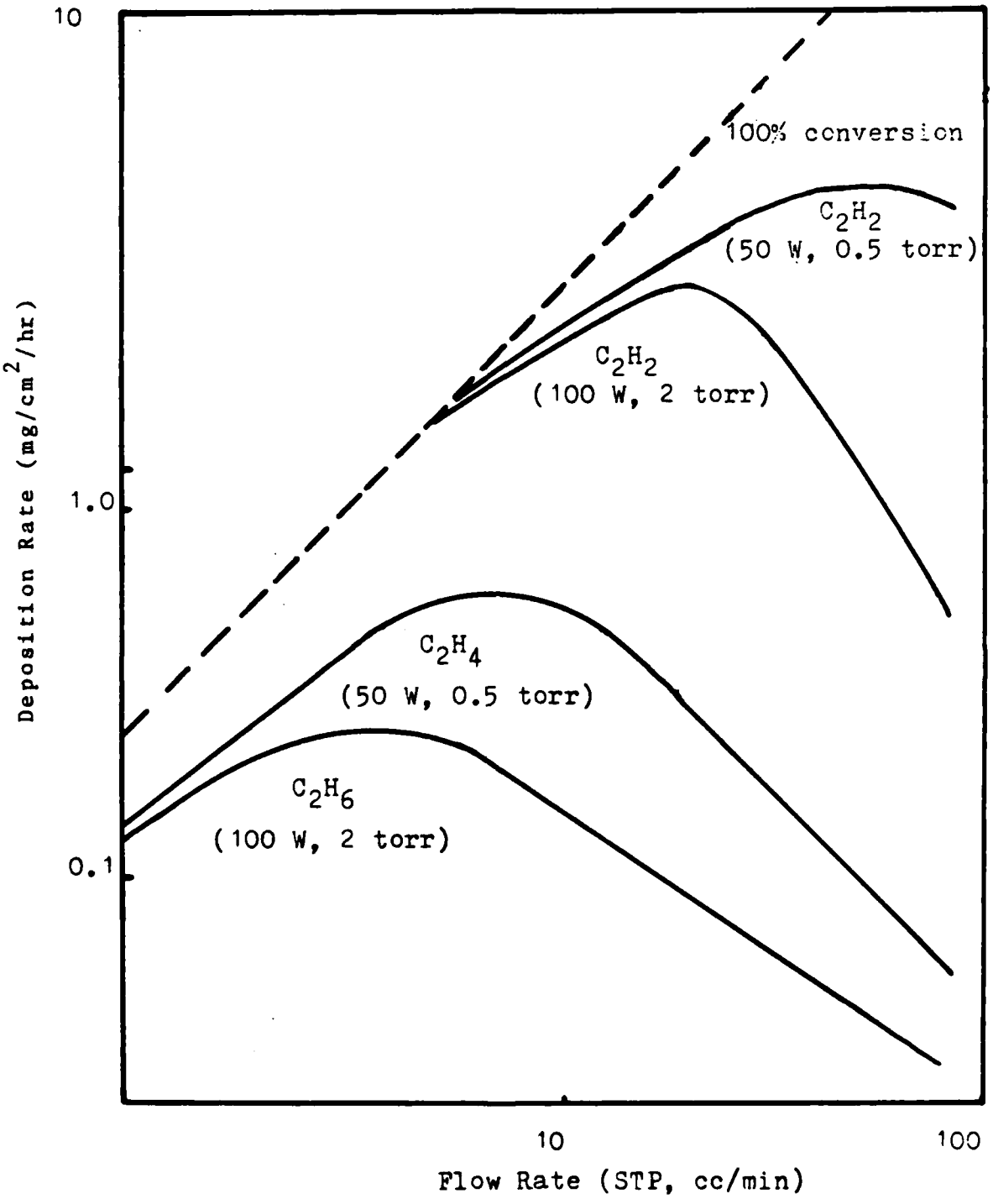

Figure 4: Rates of Plasma Polymerization of Acetylene, Ethylene and Ethane as a function of Monomer Flow Rate (40).

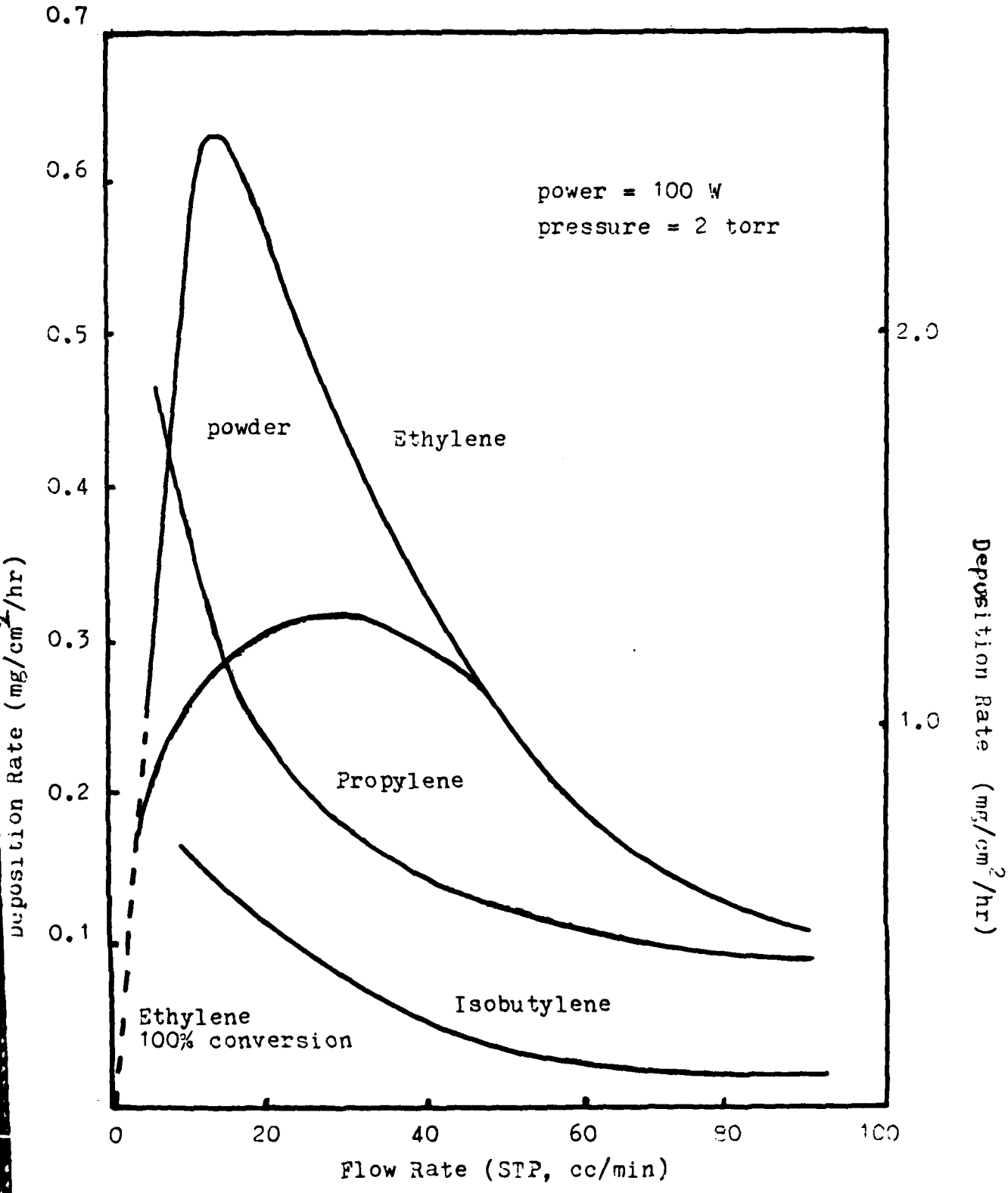

Figure 5: Rates of Plasma Polymerization of Ethylene, Propylene and Isobutylene as a function of Monomer Flow Rate (40).

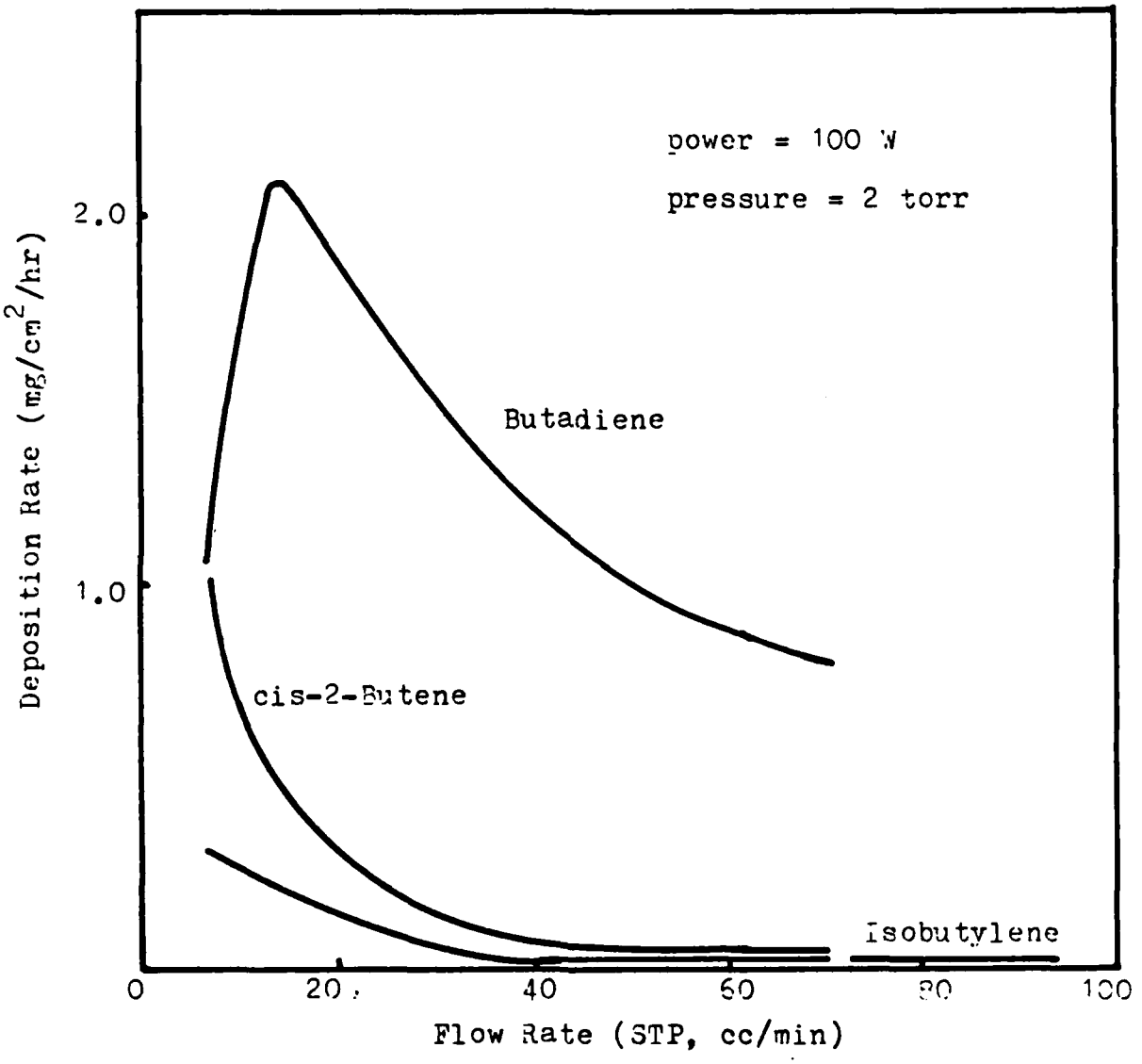

Figure 6: Rates of Plasma Polymerization of Butadiene, Cis-2-Butene and Isobutylene as a function of Monomer Flow Rate (40).

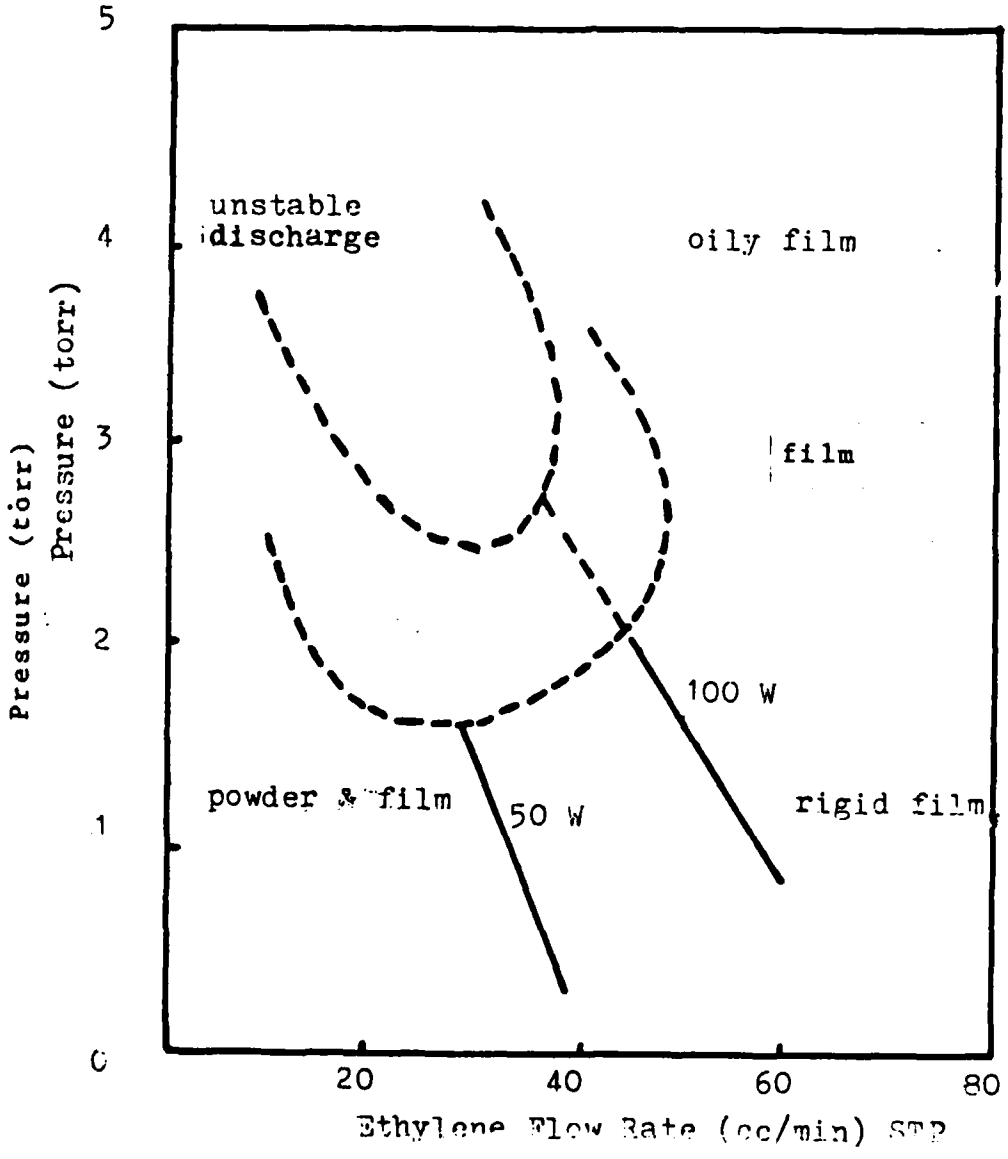

Figure 7: Characteristic Map for Plasma Polymerization of Ethylene (40)

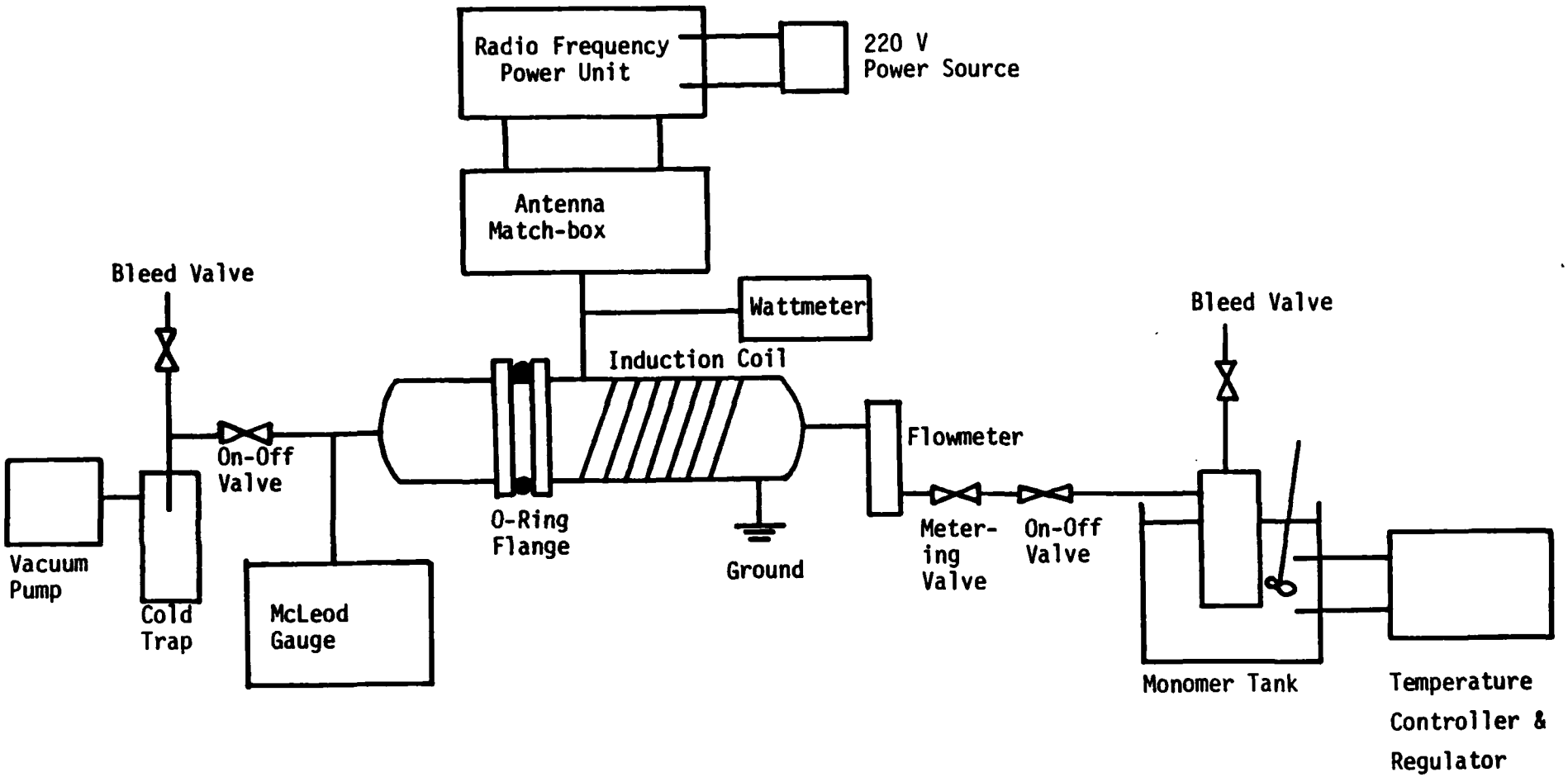

Figure 8: Schematic Diagram of the Plasma Treatment Set-up.

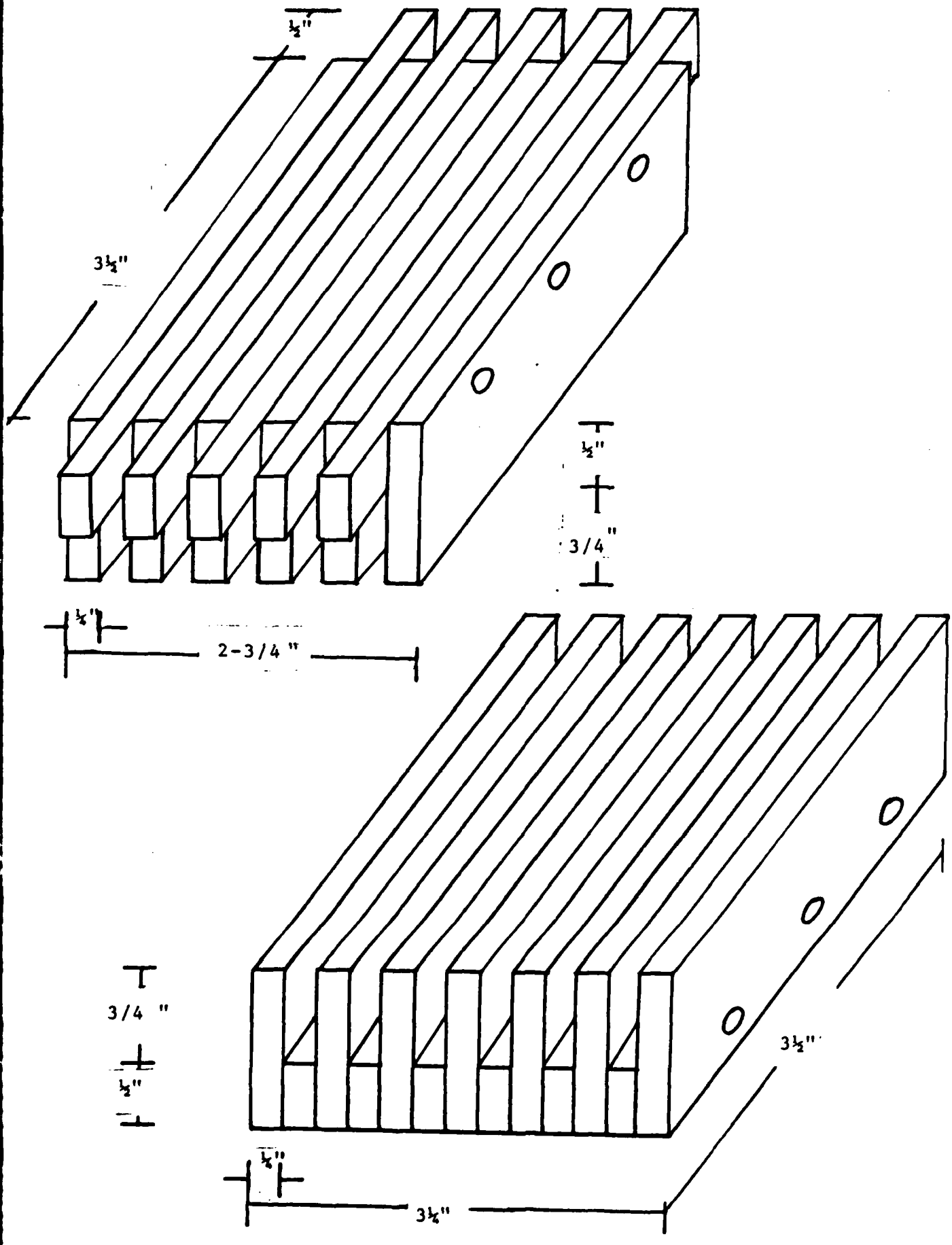

Figure 9: Diagram of the Compression Mold for Fabrication of Composite.

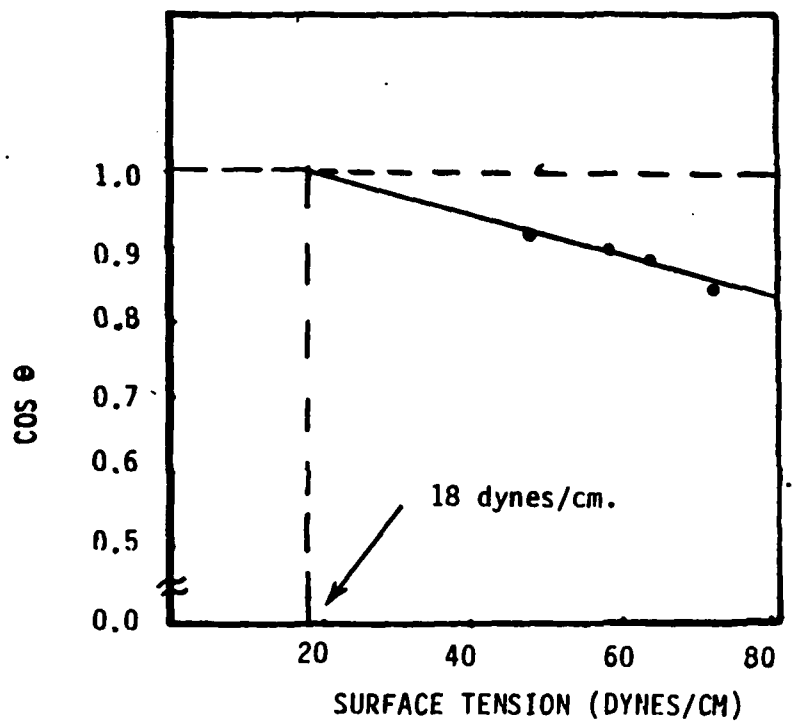

Figure 10: Determination of the Critical Surface Energy for Wetting, γ_c, of Glass Slide.

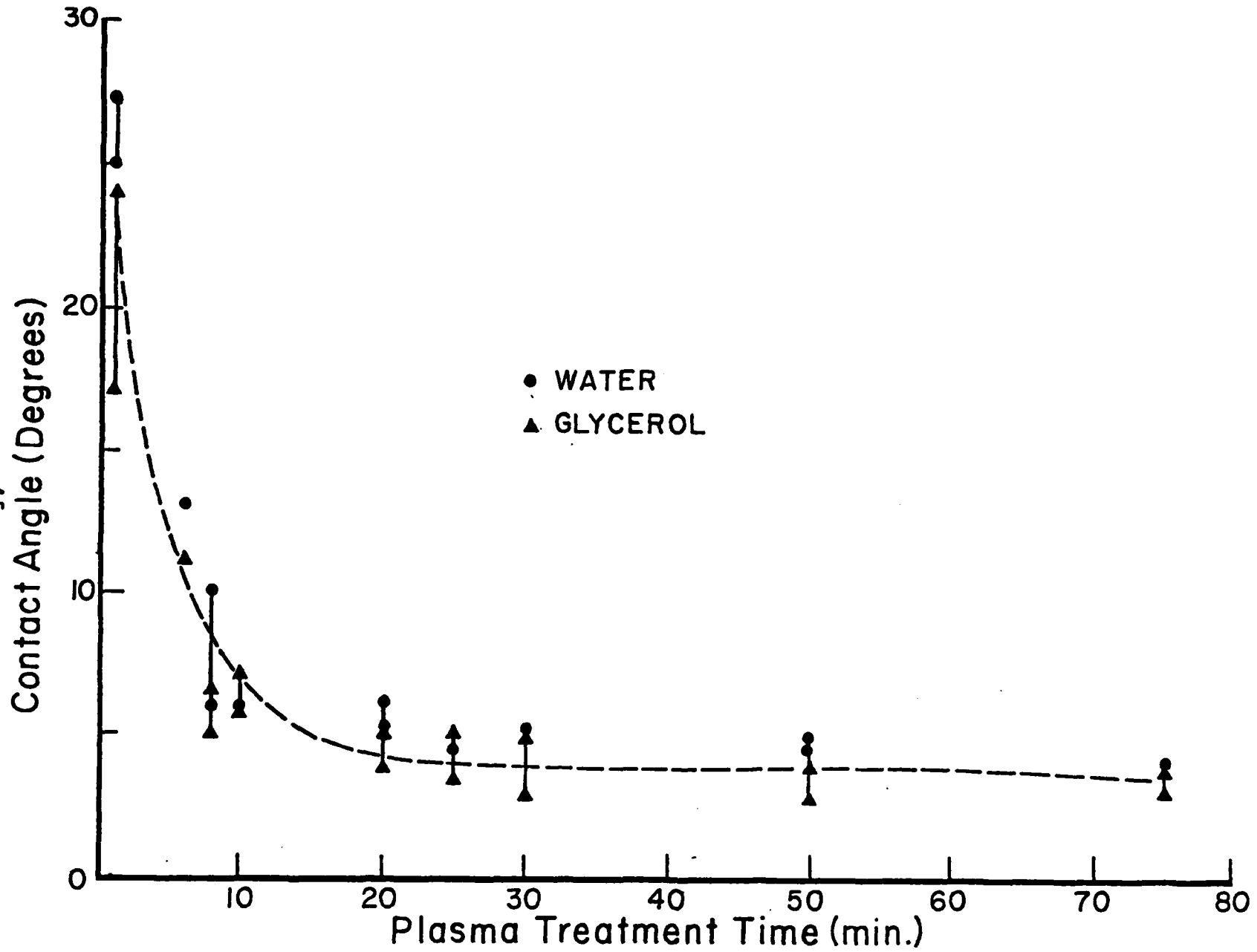

Figure 11: Contact Angle Change as a function of Plasma Treatment Time on Glass Slide.

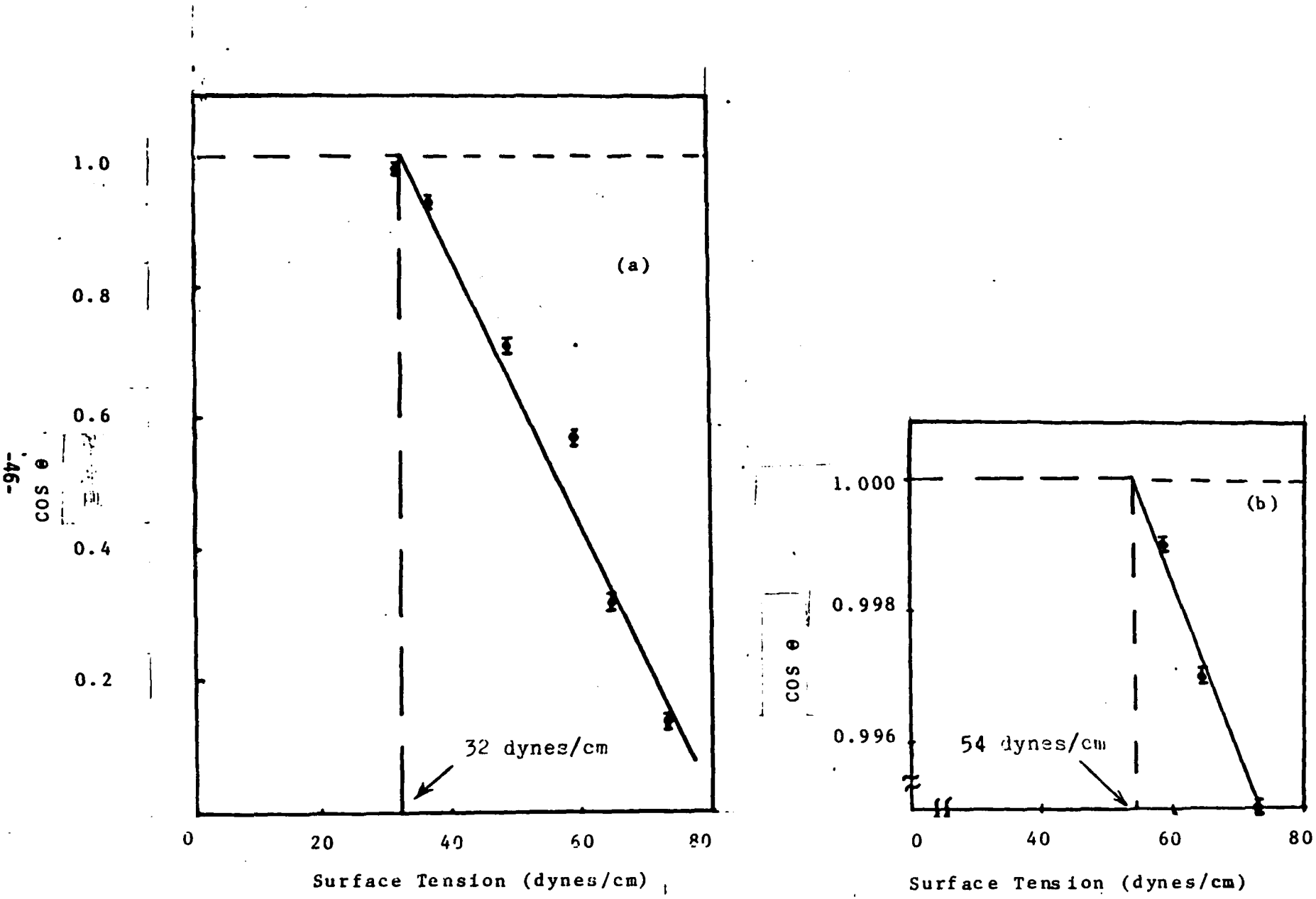

Figure 12: Critical Surface Energy of Untreated (a) and AN Plasma Treated (b) Pyrolytic Graphite

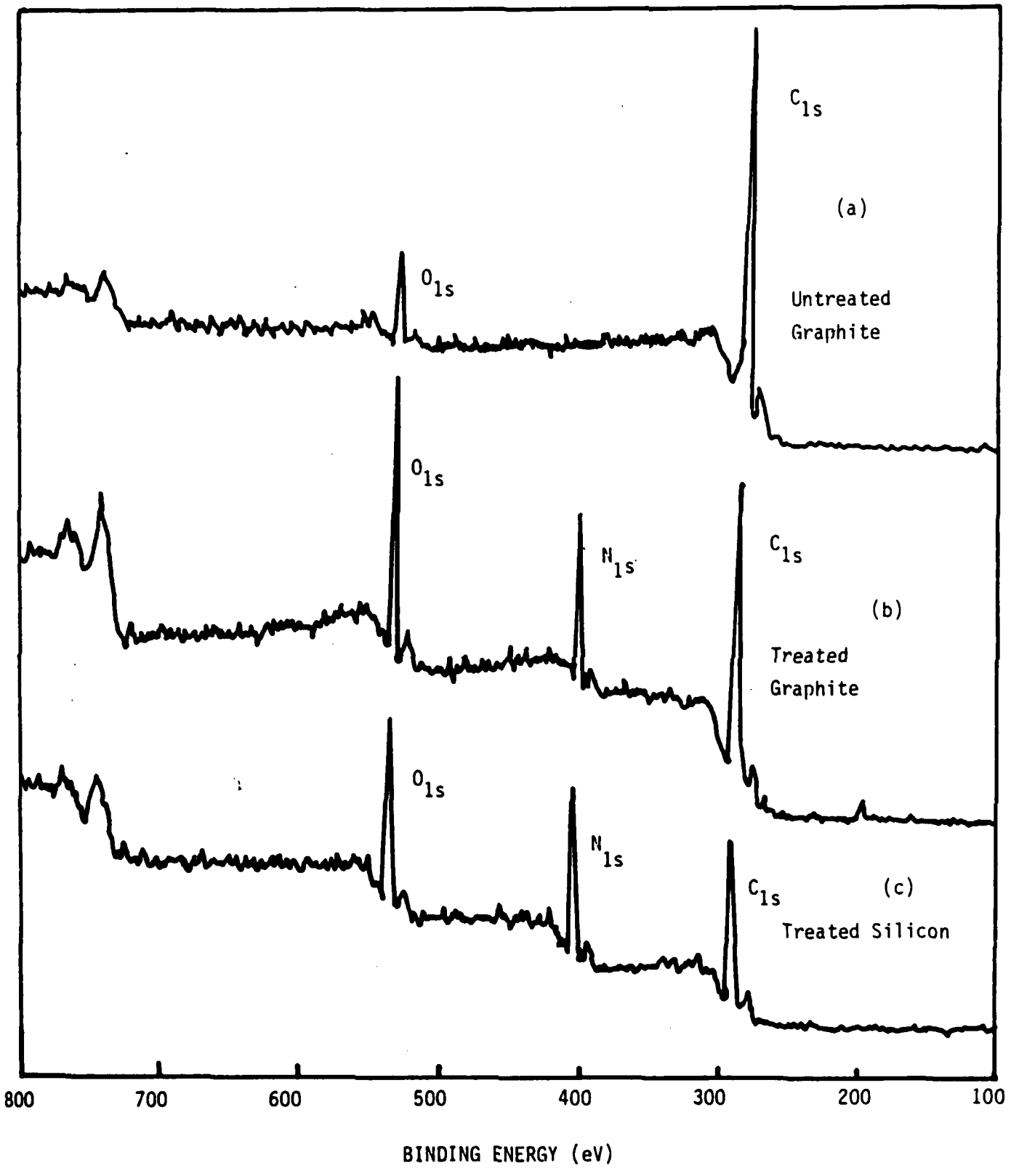

Figure 13: ESCA Spectra of Untreated (a) and Treated (b) Graphite Blocks and Treated Silicon (c) Surfaces (Treated with Acrylonitrile Plasma)

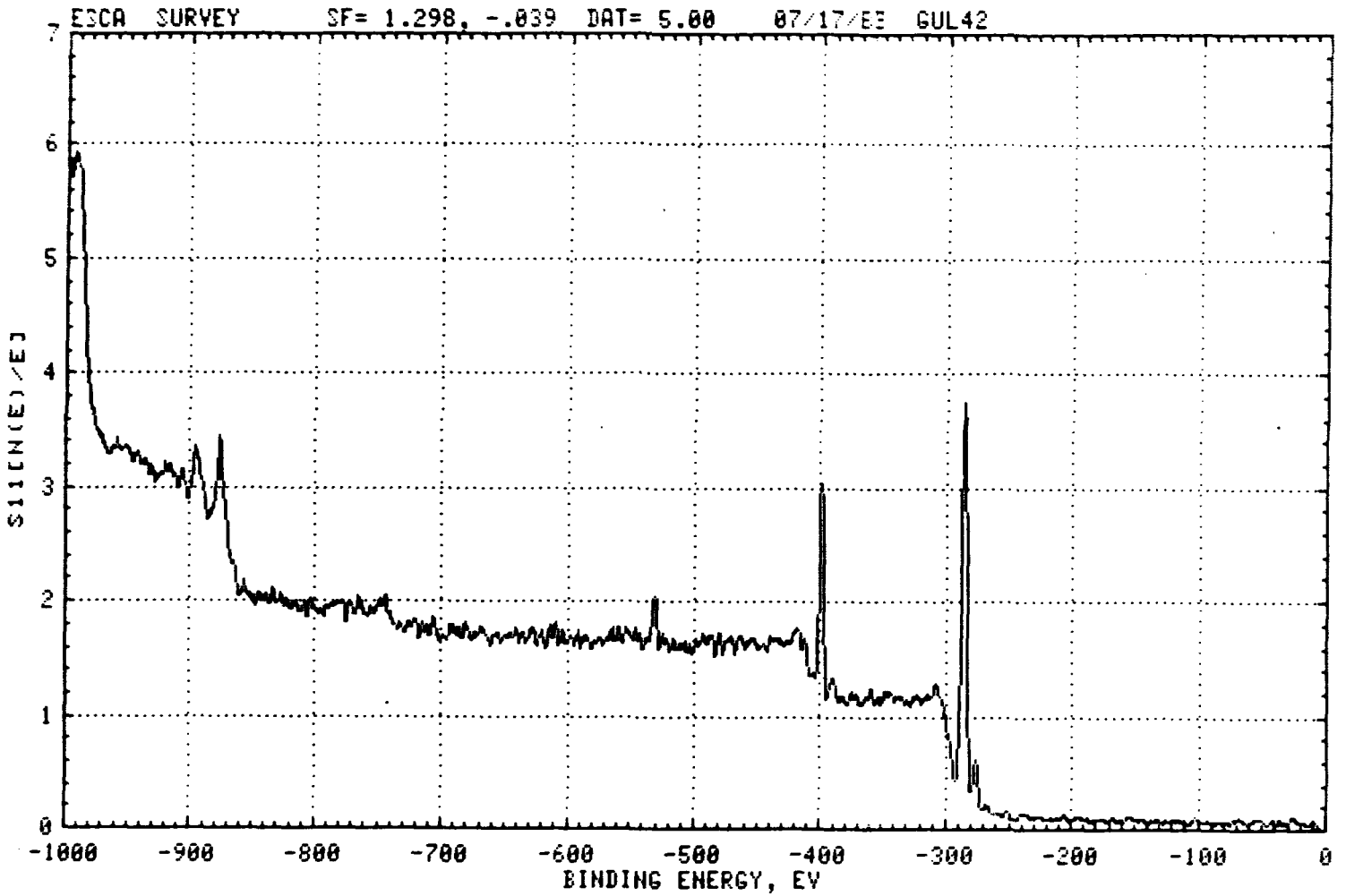

Figure 14: ESCA Spectra of Polyacrylonitrile.

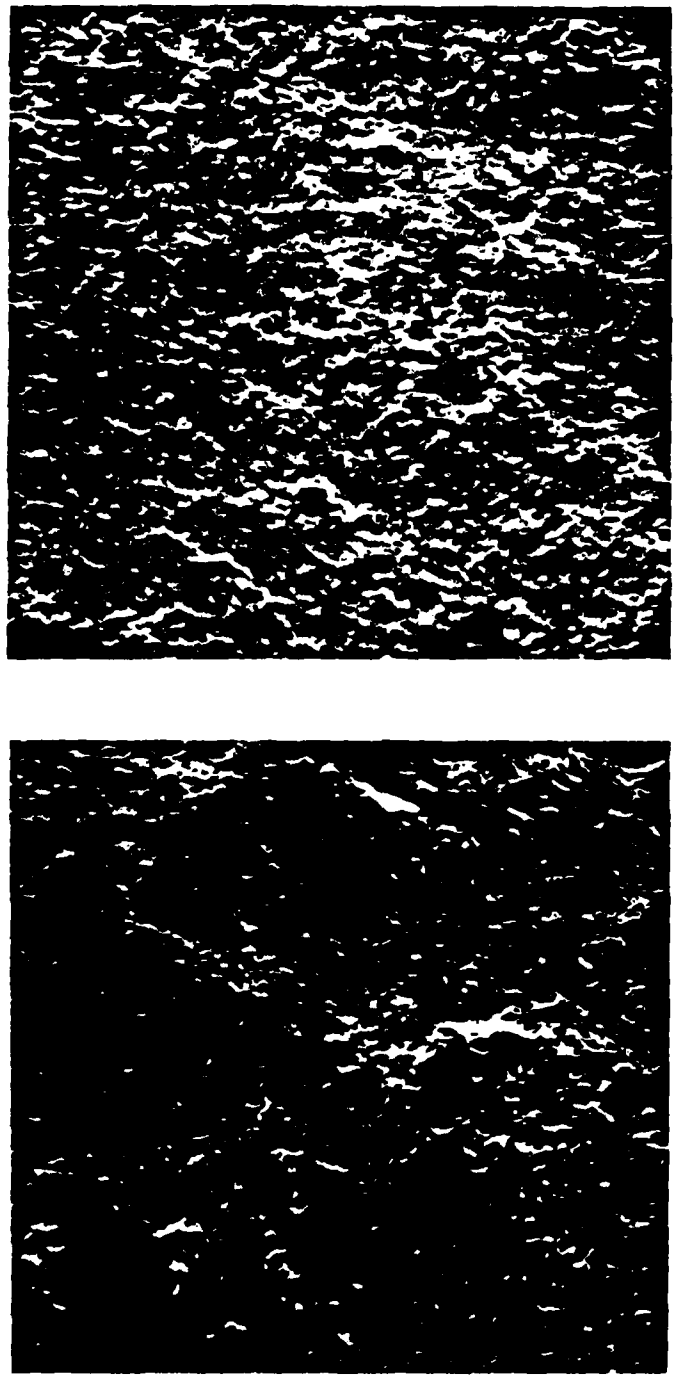

(a)

(b)

Figure 15: SEM Micrographs of Pyrolytic Graphite Surfaces, Untreated (a) and treated (b) with AN Plasma (Magnification 10000X)

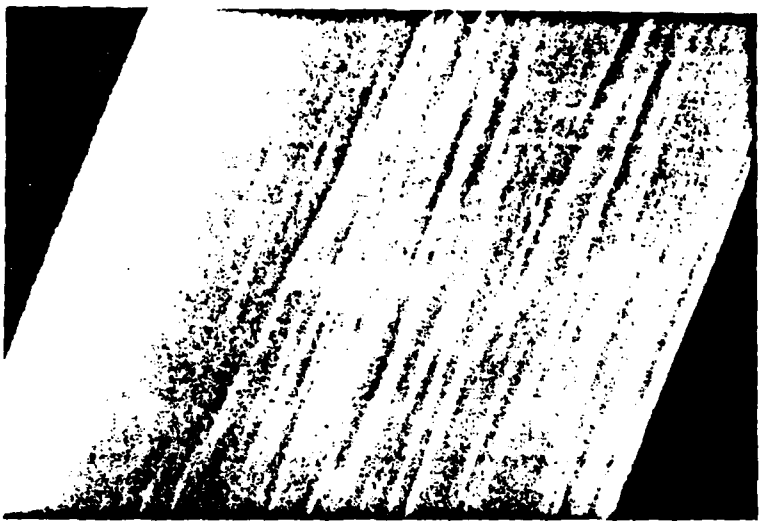

(a)

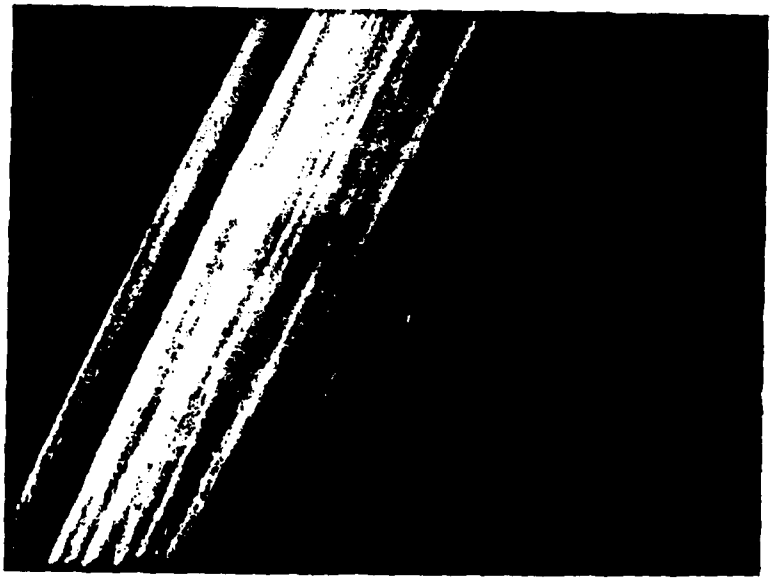

(b)

Figure 16: SEM Micrographs of Fortafil 3 Graphite Fibers, Untreated (a) and Treated (b), with Acrylonitrile Plasma (Magnifications are 8000X and 7000X respectively).

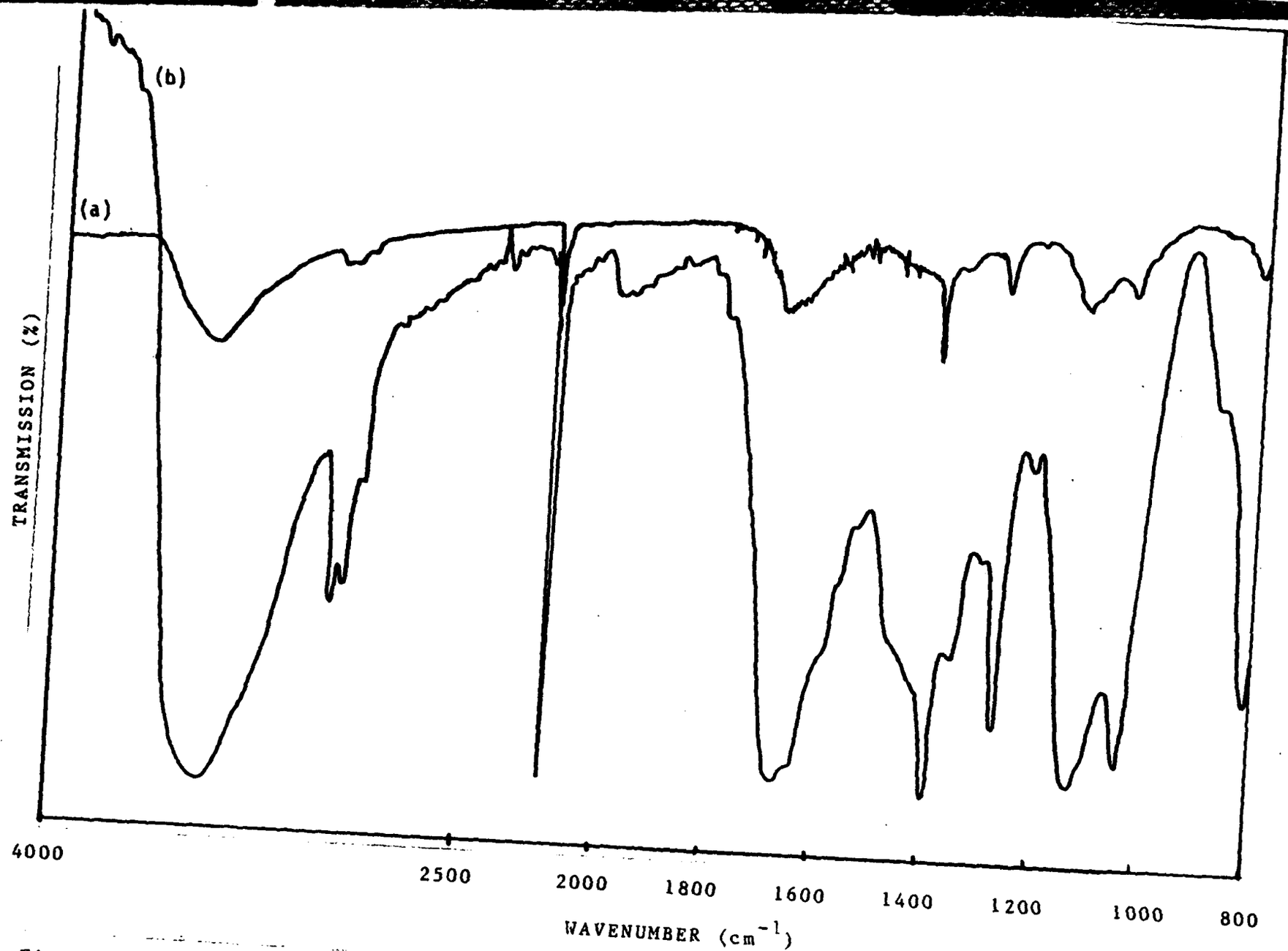

Figure 17: IR Spectra of Plasma Polyacrylonitrile on KBr Substrate (a), (b) is the Expanded Spectra.

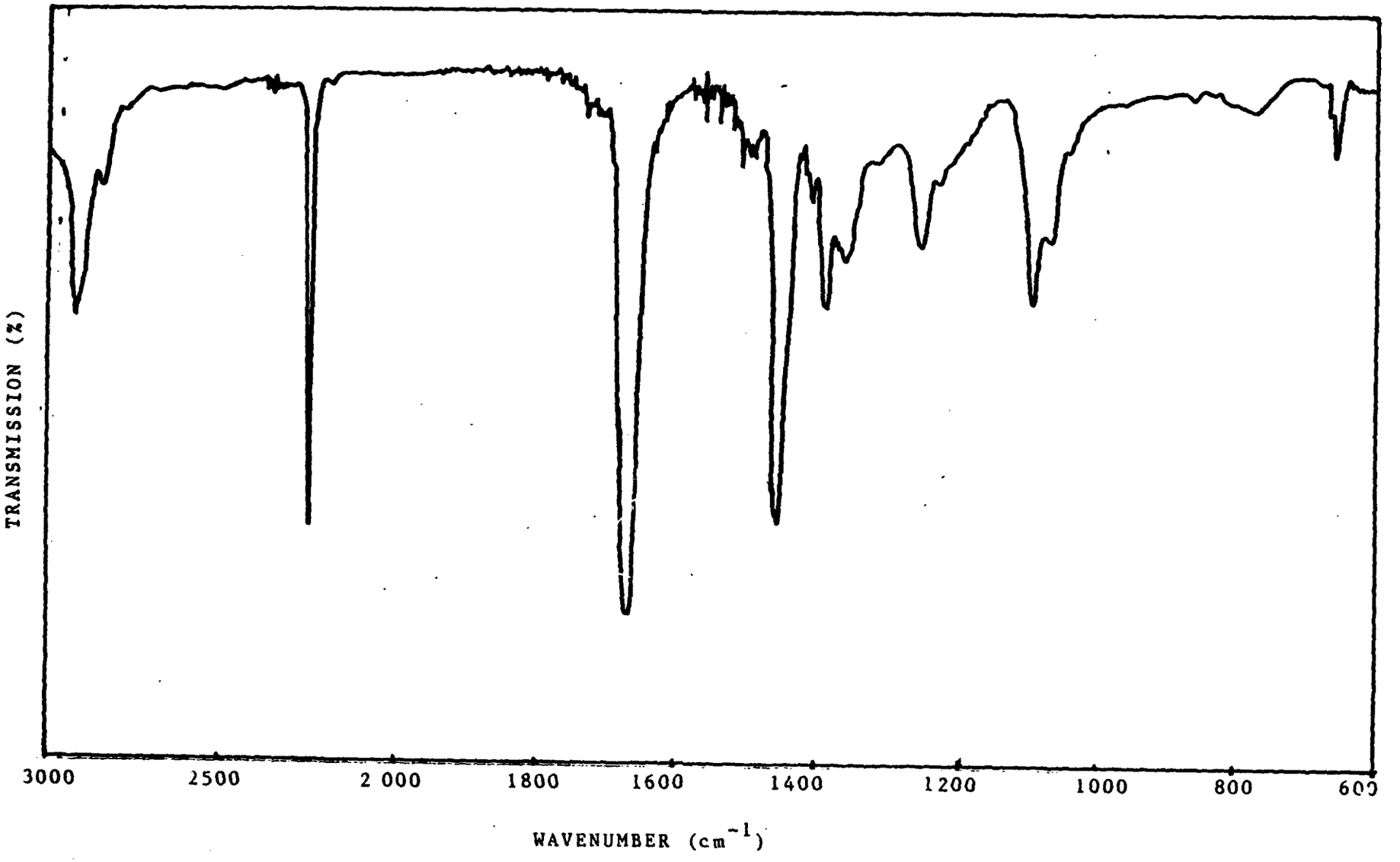
TRANSMISSION (%)
3000
2500
2 000
1800
1600
1400
1200
1000
800
600
WAVENUMBER (cm^{-1})

APPENDIX

Material Properties

Celion® carbon fibers

GY-70

CELION® GY-70 is an Ultra High Modulus Carbon Fiber unidirectional tape for use as reinforcement in high performance composites. Suggested applications include stiffness critical structures, near zero coefficient of thermal expansion laminates and other applications where the thermal, electrical or frictional properties of a highly graphitic fiber can be used to advantage.

CELION GY-70 is made from polyacrylonitrile (PAN) precursor and is processed at temperatures above 3000°C to achieve a high degree of graphitization. This results in a carbon fiber with a superior modulus and electrical/thermal conductivity surpassing other carbon fibers. Thermal and oxidative stability are also exceptionally good. The surface is treated to improve adhesion to organic polymers.

	U.S.		International	
Fiber Properties	Typical	Minimum	Typical	Minimum
Tensile Strength*	270×10^3 psi	220×10^3 psi	1860MPa	1516MPa
Tensile Modulus*	75×10^6 psi	70×10^6 psi	517GPa	482GPa
Tensile Elongation*	0.38%		0.38%	
Density	0.071 lb/in^3	0.069 lb/in^3	1.96 g/cm^3	1.90 g/cm^3
Electrical Resistivity	3900 Ω mil-ft		650μ Ω cm	

Filament and Tape Characteristics and Configuration

Filament Diameter	0.33×10^{-3} in	8.4×10^{-6} m
Cross Section	Bilobal	Bilobal
Filaments per Tow	384	384
Twist	25 turns/m	20 turns/m
Tape Width	24 in	7 cm
Number of Plies	304	304
Tape Thickness	21 mils	6.4 mm
Areal Weight	29 g/m^2	12 g/m

* Typical tensile properties of a single weight of resin

CELANESE
STRUCTURAL COMPOSITES

echnical
ata Sheet

Great
Lakes
Carbon

Fortafil 3

Fortafil® 3

Fortafil® 3 is a high strength, intermediate modulus carbon fiber supplied as either a 50,000 or 200,000 filament continuous tow with no twist. This grade is surface treated to increase the fiber-to-resin interfacial bond strength.

Typical Fiber or Tow Properties

Tensile Strength	420 ksi.	2895 MPa
Tensile Modulus	30 Msi.	207 GPa
Density	0.0625 lbs/in^3	1.73 g/cm^3
Single Filament Diameter	0.0003 in.	7.5$_u$
Tow Cross Sectional Area	0.0035 in^2	0.0226 cm^2
Tow Yield	400 ft/lb.	3.72 g/m
Electrical Conductivity	570 ohm^{-1} cm^{-1}	
Specific Heat	0.22 cal/g/°C.	
Axial Coefficient of Thermal Expansion	-0.11 x 10^{-6}/°C.	
Axial Thermal Conductivity	0.20 W/cm°C.	

Typical Unidirectional Composite Properties

In a Typical Epoxy @ 60% Fiber Volume		
Flexural Strength	250 ksi.	1724 MPa
Flexural Modulus	17 Msi.	117 GPa
Shear Strength (4:1 short beam)	15 ksi.	103 MPa

Further information may be obtained by calling (716) 278-8744.

Revised June 81

END

7-87

DTIC